

# Hepatocyte-Specific Deletion of TIPARP, a Negative Regulator of the Aryl Hydrocarbon Receptor, Is Sufficient to Increase Sensitivity to Dioxin-Induced Wasting Syndrome

David Hutin,\* Laura Tamblyn,\* Alvin Gomez,\* Giulia Grimaldi,\* Helen Soedling,\* Tiffany Cho,\* Shaimaa Ahmed,\* Christin Lucas,<sup>†</sup> Chakravarthi Kanduri,<sup>‡</sup> Denis M. Grant,\* and Jason Matthews\*,<sup>†,1</sup>

\*Department of Pharmacology and Toxicology, University of Toronto, Toronto, Canada; <sup>†</sup>Department of Nutrition, Institute of Basic Medical Sciences, University of Oslo, Oslo, Norway; and <sup>‡</sup>Department of Informatics, Jebsen Centre of Excellence for Celiac Disease Research, University of Oslo, Oslo, Norway

<sup>1</sup>To whom correspondence should be addressed at Department of Nutrition, Institute of Basic Medical Sciences, University of Oslo, Sognsvannsveien 9, 0372 Oslo, Norway. Fax: +4722851398; E-mail: jason.matthews@medisin.uio.no.

## ABSTRACT

The aryl hydrocarbon receptor (AHR) mediates the toxic effects of dioxin (2, 3, 7, 8-tetrachlorodibenzo-*p*-dioxin; TCDD), which includes thymic atrophy, steatohepatitis, and a lethal wasting syndrome in laboratory rodents. Although the mechanisms of dioxin toxicity remain unknown, AHR signaling in hepatocytes is necessary for dioxin-induced liver toxicity. We previously reported that loss of TCDD-inducible poly(adenosine diphosphate [ADP]-ribose) polymerase (TIPARP/PARP7/ARTD14), an AHR target gene and mono-ADP-ribosyltransferase, increases the sensitivity of mice to dioxin-induced toxicities. To test the hypothesis that TIPARP is a negative regulator of AHR signaling in hepatocytes, we generated *Tiparp*<sup>fl/fl</sup> mice in which exon 3 of *Tiparp* is flanked by loxP sites, followed by Cre-lox technology to create hepatocyte-specific (*Tiparp*<sup>fl/fl</sup>Cre<sup>Alb</sup>) and whole-body (*Tiparp*<sup>fl/fl</sup>Cre<sup>CMV</sup>, *Tiparp*<sup>Ex3-/-</sup>) *Tiparp* null mice. *Tiparp*<sup>fl/fl</sup>Cre<sup>Alb</sup> and *Tiparp*<sup>Ex3-/-</sup> mice given a single injection of 10 μg/kg dioxin did not survive beyond days 7 and 9, respectively, while all *Tiparp*<sup>+/+</sup> mice survived the 30-day treatment. Dioxin-exposed *Tiparp*<sup>fl/fl</sup>Cre<sup>Alb</sup> and *Tiparp*<sup>Ex3-/-</sup> mice had increased steatohepatitis and hepatotoxicity as indicated by greater staining of neutral lipids and serum alanine aminotransferase activity than similarly treated wild-type mice. *Tiparp*<sup>fl/fl</sup>Cre<sup>Alb</sup> and *Tiparp*<sup>Ex3-/-</sup> mice exhibited augmented AHR signaling, denoted by increased dioxin-induced gene expression. Metabolomic studies revealed alterations in lipid and amino acid metabolism in liver extracts from *Tiparp*<sup>fl/fl</sup>Cre<sup>Alb</sup> mice compared with wild-type mice. Taken together, these data illustrate that TIPARP is an important negative regulator of AHR activity, and that its specific loss in hepatocytes is sufficient to increase sensitivity to dioxin-induced steatohepatitis and lethality.

**Key words:** aryl hydrocarbon receptor; wasting syndrome; ADP-ribosylation; 2, 3, 7, 8-tetrachlorodibenzo-*p*-dioxin; TCDD-inducible poly-ADP-ribose polymerase.

2, 3, 7, 8-Tetrachlorodibenzo-*p*-dioxin (TCDD; dioxin) is a highly toxic environmental contaminant produced during waste incineration and other high-temperature industrial processes, and it

remains a global health concern. The toxic effects of dioxin are mediated through its binding to and activation of the aryl hydrocarbon receptor (AHR), which is a member of the basic

helix-loop-helix Period-AHR nuclear translocator (ARNT)-Single-minded family of transcription factors. In the canonical AHR signaling pathway, ligand binding to cytosolic AHR causes its translocation to the nucleus where it dimerizes with ARNT (also known as hypoxia-inducible factor 1 $\beta$ ). The AHR: ARNT heterodimer then binds DNA sequence elements (termed AHREs or DREs) located within the regulatory regions of its target genes, which include *cytochrome P4501A1* (CYP1A1), CYP1B1, and TCDD-inducible adenosine diphosphate (ADP)-ribose polymerase (TIPARP) (Ma et al., 2001; Whitlock, 1999; Zhang et al., 1998). In addition to its roles in dioxin toxicity, xenobiotic metabolism and vascular development (Stevens et al., 2009), AHR has important roles in T-cell differentiation, in the defense against bacterial infections and in gut homeostasis (Moura-Alves et al., 2014; Quintana et al., 2008). To date, >400 AHR ligands have been identified, including dietary compounds (3, 3'-diindolylmethane), various endogenous ligands (kynurenine, 6-formylindolo(3, 2b)carbazole), and environmental contaminants such as dioxin (Denison and Nagy, 2003).

Dioxin causes diverse toxic effects in laboratory rodents including immunosuppression, steatohepatitis, impaired reproduction, and a lethal wasting syndrome (Birnbau, 1994, 1995; Poland and Knutson, 1982). A single dose of dioxin induces a lethal starvation-like syndrome, which includes decreased gluconeogenesis, liver damage, steatohepatitis and dyslipidaemia, ultimately leading to lethality (Linden et al., 2010; Seefeld et al., 1984). Acute lethality varies widely both among species and between rodent strains. For example, the median lethal dose (LD<sub>50</sub>) for guinea pigs is 1–2  $\mu$ g/kg dioxin, whereas the LD<sub>50</sub> for hamsters is >5000  $\mu$ g/kg (Pohjanvirta and Tuomisto, 1994; Poland and Knutson, 1982). In most strains of mice, lethality occurs only 2–3 weeks after a single dose of 115–300  $\mu$ g/kg of dioxin (Pohjanvirta and Tuomisto, 1994; Poland and Knutson, 1982). There is a roughly 10-fold difference in susceptibility between the high sensitivity C57BL/6 (Ahr<sup>b1</sup> allele) and low sensitivity DBA/2 (Ahr<sup>d</sup> allele) mouse strains, which is due to polymorphic variations in their ligand-binding domains (Poland et al., 1994). The molecular mechanisms of dioxin-induced wasting syndrome remain obscure, but transgenic mice overexpressing AHR show increased sensitivity to dioxin toxicities, whereas Ahr<sup>-/-</sup> null and Ahr<sup>dbd</sup> mice, which express a mutant AHR that does not bind to AHREs, are resistant to the effects of dioxin (Fernandez-Salguero et al., 1996; Lee et al., 2010; Walisser et al., 2005).

TIPARP (PARP7/ARTD14) is an AHR-regulated gene and a member of the poly-adenosine diphosphate (ADP)-ribose polymerase (PARP) family. PARPs are nicotinamide adenine dinucleotide (NAD<sup>+</sup>)-dependent enzymes that use NAD<sup>+</sup> as a substrate to transfer 1 molecule of ADP-ribose, referred to as mono-ADP-ribosylation (MARylation), or several ADP-ribose moieties, referred to as poly-ADP-ribosylation (PARylation), to specific amino acid residues on themselves and on target proteins (Hottiger et al., 2010). Mono- and poly-ADP-ribosylation are reversible posttranslational modifications involved in several biological processes, such as immune cell function, regulation of transcription, protein expression and DNA repair (Kraus and Hottiger, 2013). We previously reported that TIPARP is a mono-ADP-ribosyltransferase that functions as part of a negative feedback loop to repress AHR activity through a mechanism that involves reduced ligand-induced AHR protein levels and that requires TIPARP's catalytic activity (MacPherson et al., 2013). Moreover, Tiparp<sup>-/-</sup> mice exhibit increased AHR activity but also increased sensitivity to dioxin-induced toxicities, including steatohepatitis, hepatotoxicity and lethal wasting syndrome

(Ahmed et al., 2015). Although the mechanisms of dioxin-induced toxicity remain incompletely understood, AHR expression in hepatocytes is needed to generate the adaptive as well as toxic response to dioxin exposure (Walisser et al., 2005).

Here, we describe the generation of Tiparp conditional mutant mice in which exon 3 of the Tiparp gene is flanked by loxP sites, and the subsequent creation of both hepatocyte-specific (Tiparp<sup>fl/fl</sup>Cre<sup>Alb</sup>) and whole-body (Tiparp<sup>fl/fl</sup>Cre<sup>CMV</sup>; Tiparp<sup>Ex3-/-</sup>) TIPARP knockout mice. These mice were used to further investigate the role of TIPARP in AHR signaling and dioxin-induced toxicity.

## MATERIALS AND METHODS

**Generation of conditional Tiparp null mice.** Tiparp<sup>fl/fl</sup> mice, where exon 3 of Tiparp was flanked by loxP sites, were generated from embryonic stem (ES) cells purchased from European Conditional Mouse Mutagenesis (EUCOMM; Tiparp<sup>tm1a</sup>(EUCOMM)<sup>Wtsi</sup>). ES cells were expanded by the Toronto Centre for Phenogenomics (TCP). Correct targeted recombination was confirmed in 2 of 5 ES cell clones purchased. Briefly, SphI-digested genomic DNA was used in Southern blotting to produce 8.9 kb (wild-type [WT]) and 12.3 kb (tm1a) fragments spanning the 5' region of the targeted sequence of Tiparp, and in the targeted allele, including the neomycin-resistance (Neo) cassette. The Neo probe was used to reveal additional or random integrations of the targeting vector in the genomes (fragments of incorrect sizes); these ES clones were excluded. PCR primers used to generate the respective probes are provided in Supplementary Table 1. Based on the positive Southern blot results, ES cell clones D3 and G3 were chosen for aggregation and implantation into pseudopregnant surrogate females (performed by TCP). Chimeric Tiparp<sup>+/tm1a</sup> mice were bred to C57BL/6 albino females and pups were genotyped to identify those with germline transmission of the conditional mutant Tiparp allele (Tiparp<sup>+/tm1a</sup>); only ES clone G3 resulted in successful germline transmission. Some Tiparp<sup>+/tm1a</sup> mice were bred to B6.C-Tg(CMV-cre)1Cgn/J (Jackson Labs, Bar Harbor, Maine) to remove the Neo cassette and the targeted exon and leave the lacZ reporter gene (conversion to tm1b allele) and then outbred once to C57BL/6N to remove Tg-(CMV-cre). Mice heterozygous for the tm1b allele were then intercrossed to make homozygous tm1b mice (Tiparp<sup>tm1b/tm1b</sup>, referred to as Tiparp<sup>Ex3-/-</sup>). Other Tiparp<sup>+/tm1a</sup> mice were bred to B6(C3)-Tg(Pgk1-FLPo)10Sykr/J (Jackson Labs) to remove the lacZ and Neo cassettes and leave the targeted exon flanked by LoxP sites (conversion to tm1c allele) and then outbred once to C57BL/6N to remove Tg-(Pgk1-FLPo) (Tiparp<sup>+/tm1c</sup>). Tiparp<sup>+/tm1c</sup> mice were bred to B6.C-Tg(CMV-cre)1Cgn/J to remove the targeted exon (conversion to tm1d allele) and then outbred once to C57BL/6N to remove Tg-(CMV-cre). Mice heterozygous for the tm1d allele were then intercrossed to make homozygous tm1d mice (Tiparp<sup>tm1d/tm1d</sup>, referred to as Tiparp<sup>Ex3-/-</sup>). Tiparp<sup>+/tm1c</sup> mice were also bred to B6N.Cg-Tg(Alb-cre)21Mgn/J (Jackson Labs) to create hepatocyte-specific Tiparp knock-out mice (Tiparp<sup>tm1c/tm1c</sup>Cre<sup>Alb</sup>), referred to as Tiparp<sup>fl/fl</sup>Cre<sup>Alb</sup>. This colony was maintained such that Tiparp<sup>fl/fl</sup> female mice were paired with Tiparp<sup>fl/fl</sup>Cre<sup>Alb</sup> male mice. Genotypes of all mice were determined by PCR analysis of tail biopsies using PCR primers shown in Supplementary Table 1. The specificity of excision events in Tiparp<sup>fl/fl</sup>Cre<sup>Alb</sup> mice was determined by quantitative real time PCR (qPCR) using primer pairs specific for exon 3 of Tiparp compared with primer pairs specific for intron 1 (Supplementary Table 1). Genotype controls used in experiments for the Tiparp<sup>fl/fl</sup>Cre<sup>Alb</sup> line are Tiparp<sup>fl/fl</sup> (observed to

be phenotypically equivalent to WT mice), and for the *Tiparp*<sup>Ex3-/-</sup> are *Tiparp*<sup>+/+</sup>. Both *tm1b* and *tm1d* lines were used.

**In vivo dioxin treatment studies.** All experiments used 8- to 10-week-old male mice. For the acute 6 h exposure studies, *Tiparp*<sup>Ex3-/-</sup> or *Tiparp*<sup>fl/fl</sup>*Cre*<sup>Alb</sup> mice and their respective strain-specific WT control mice were treated with a single intraperitoneal (i.p.) injection of 100 µg/kg dioxin, and livers were excised and flash frozen 6 h later. For the subacute dioxin toxicity studies, mice were treated with a single i.p. injection of 10 or 100 µg/kg of dioxin and sacrificed on day 6. The 10 µg/kg dose of dioxin was dissolved in a mixture of corn oil and dimethyl sulfoxide (CO:DMSO; 90:10, referred to as CO), while the 100 µg/kg dose of dioxin was dissolved in pure DMSO. For the survival studies, mice were followed for up to 30 days after a single injection of 10 or 100 µg/kg of dioxin. Control mice received equivalent weight-adjusted volumes of CO or DMSO. The time point for euthanization was determined based on endpoint criteria for our study: a loss of 20% body weight or indications of acute distress. All control mice were euthanized to match the endpoints of dioxin-sensitive mice. For food intake studies, mice were housed individually and provided intact pellets of food that were weighed daily; a baseline was determined for each mouse by monitoring for 1 week prior to treatment as described previously (Ahmed et al., 2015). Whole blood was obtained from the saphenous vein for serum alanine aminotransferase (ALT) analysis as described previously in Ahmed et al. (2015). Hepatic glycogen levels were determined from 10 mg of frozen liver using the Glycogen Assay Kit II (Abcam). Liver, thymus, white and brown adipose tissue (WAT and BAT) were dissected and weighed. Livers from *Tiparp*<sup>Ex3-/-</sup> or *Tiparp*<sup>fl/fl</sup>*Cre*<sup>Alb</sup> mice treated with vehicle, 10 or 100 µg/kg dioxin were collected either on day 6 or on the day of euthanization in the survival studies. Care and treatment of animals followed the guidelines set by the Canadian Council on Animal Care, and all protocols were approved by the University of Toronto Animal Care Committee.

**Hepatocytes.** *Tiparp*<sup>fl/fl</sup>*Cre*<sup>Alb</sup> or *Tiparp*<sup>fl/fl</sup> male mice (8- to 10-weeks old) were used to isolate primary hepatocytes. Mouse liver was perfused with liver perfusion medium (Invitrogen) for 10 min followed by liver digestion medium for 10 min. Freshly prepared hepatocytes were seeded at a final density of  $0.5 \times 10^6$  cells/well onto type I collagen coated 6-well plates in attachment medium (William's E media, 10% dextran-coated charcoal (DCC) stripped fetal bovine serum (FBS),  $1 \times$  penicillin/streptomycin, and 10-nM insulin). The medium was changed 2 h after plating, and all experiments were performed on the second day. Ligands were added to the cells in M199 media with 5% DCC-FBS and cells were harvested 16 h after ligand treatment for RNA extraction.

**RNA extraction and gene expression analysis.** Livers were removed, washed in ice-cold PBS, weighed, and flash frozen in liquid nitrogen. Frozen livers were homogenized in TRIZOL reagent (Life Technologies) and total RNA was isolated using the Aurum RNA isolation kits (BioRad) and reverse transcribed as previously described (Ahmed et al., 2015). Primers used to amplify target transcripts are provided in Supplementary Table 1 or described elsewhere (Ahmed et al., 2015). All genes were normalized to TATA-binding protein levels and analyzed using the comparative  $C_T$  ( $\Delta\Delta C_T$ ) method.

**Chromatin immunoprecipitation (ChIP) assays.** ChIP assays were performed as previously described in Lo et al. (2011). Briefly,

approximately 100 mg of frozen mouse liver was homogenized in 1% formaldehyde in PBS and incubated for 10 min at room temperature. The homogenate was centrifuged at  $8000 \times g$  for 5 min at 4°C. Pellet was washed in ice-cold PBS, centrifuged, and resuspended in 900 µl of TSEI (20 mM Tris-HCl [pH 8.0], 150 mM NaCl, 2 mM EDTA, 1% Triton X-100, 0.1% sodium dodecyl sulfate) +  $1 \times$  Protease Inhibitor Cocktail (Sigma, St Louis, Missouri). Samples were sonicated 10 times for 30 s ON/30 s OFF on the high setting using a Bioruptor (Diagenode). The supernatants were transferred to new microcentrifuge tubes and incubated with rabbit IgG (5 µg; Sigma) and antiAHR (5 µg; SA-210, Enzo) overnight at 4°C under gentle agitation. ChIP samples were washed, the DNA and the ChIP-qPCR was performed as previously described in Lo et al. (2011).

**Histology.** Hematoxylin and eosin and Oil-Red-O/Hematoxylin staining were performed following standard methods with representative images provided. Paraformaldehyde-fixed or optimal cutting temperature (OCT) compound-embedded tissues were provided to the Histology Core Facility at the Princess Margaret Cancer Centre, Toronto, Ontario, for all histology sample processing, staining and scanning of stained slides.

**Western blotting.** For hepatic AHR protein detection, whole cell extracts were prepared by homogenizing 100 mg of liver tissue in RIPA lysis buffer. Ten micrograms of total protein were separated by SDS-PAGE and transferred to a nitrocellulose membrane. Membranes were incubated with antiAHR antibody (SA-210) and stripped and then incubated with antiβ-actin antibody (Sigma A-2228).

**Metabolomics.** *Tiparp*<sup>fl/fl</sup> and *Tiparp*<sup>fl/fl</sup>*Cre*<sup>Alb</sup> mice were treated with a single intraperitoneal injection of CO: DMSO or 10 µg/kg dioxin. Liver tissue (100 mg) was collected on day 3 and flash frozen in liquid nitrogen. The frozen tissue was extracted and metabolomic analyses were performed by Metabolon (Durham, North Carolina). Raw data received from Metabolon were preprocessed to input missing values and normalized using logarithmic transformation. Shapiro's test was used to test for normality and Levene's test was used to test for the homogeneity of variances. Analysis of variance (ANOVA) was used to analyze the differences in group means, followed by Tukey's-HSD for post hoc correction. The FDR method was used to adjust the *p*-values for multiple ANOVA tests (one for each metabolite). At an FDR of 10%, all the group comparisons that exhibited a statistically significant difference (post hoc corrected *p*-values < .05) were considered significant. All the analyses were performed in R version 3.4.1.

**Statistical analysis.** All data were presented as means and SEM. Two-way ANOVA followed by Sidak's post hoc test or 1-way ANOVA followed by Tukey's post hoc test were used to assess statistical significance (*p* < .05) using GraphPad Prism 6 Software (San Diego, California) or R version 3.4.1.

## RESULTS

### Generation of Conditional *Tiparp*<sup>fl/fl</sup> Mice

Mice harboring the conditional *Tiparp*<sup>fl</sup> allele were generated from *Tiparp*<sup>tm1a(EUCOMM)Wtsi</sup> ES cells purchased from EUCOMM. A partial map of both the *Tiparp* WT and *Tiparp* *tm1a* alleles is shown in Figure 1A. Southern blotting of genomic DNA isolated from 4 different ES cell clones confirmed the correct integration of the *tm1a* allele in the ES cell clones D3 and G3 (Figure 1B).



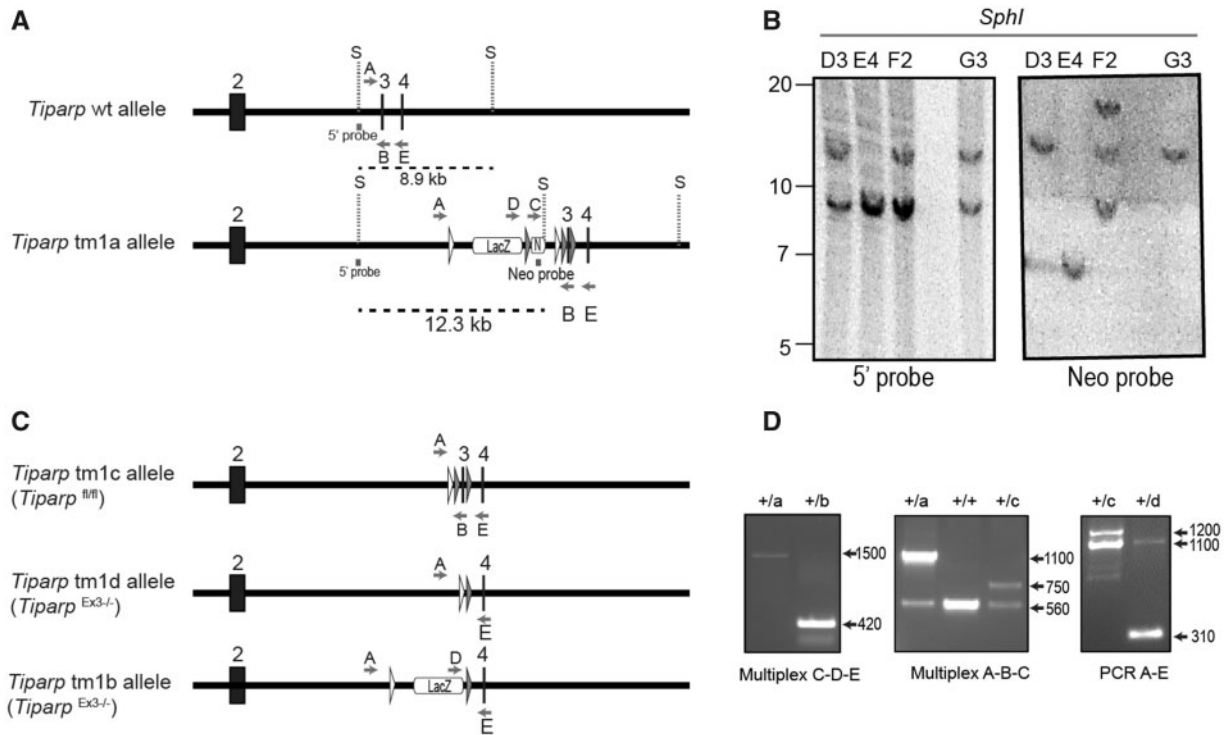


**Figure 1.** Generation of the conditional *Tiparp*<sup>fl/fl</sup> mice. **A**, Schematic diagram of *Tiparp* WT allele and the allele with successful recombination of the tm1 targeting construct (*Tiparp* tm1a allele) and corresponding Southern blot data. Exon numbers reflect known coding exons; white arrowheads represent FRT sites; gray arrowheads represent LoxP sites; LacZ represents lacZ reporter gene; N represents the Neo resistance cassette; S, SphI site; dashed lines indicate the fragment of DNA generated by SphI digestion that was detected with the radiolabeled probes (5' probe and Neo probe); letters indicate genotyping primers. **B**, Southern blots show *Tiparp* allele fragments detected with the radiolabeled probes: ES clones D3 and G3 show correct homologous recombination of the targeting construct (12.3 kb fragment detected with 5' probe) without additional random integrations (only the 12.3 kb band detected with Neo probe). **C**, Schematic diagram of *Tiparp* tm1 alleles following excision of sequence by CRE or FLP recombinases. **D**, PCR data from mouse tail biopsies. The *Tiparp* tm1a allele was converted to tm1b using CRE recombinase to remove the Neo cassette and exon 3 located between the LoxP sites. Primer pair D-E amplifies a product spanning the excision sites to show that the floxed sequences were removed (420 bp). The *Tiparp* tm1a allele was converted to tm1c using FLP recombinase to remove the LacZ and Neo cassettes located between the FRT sites. Primer pair A-B amplifies a product spanning the excision site to show that the sequence was flipped out (750 bp). The *Tiparp* tm1c allele was converted to tm1d using CRE recombinase to remove the floxed exon 3. Primer pair A-E amplifies a product spanning the floxed region to show that the exon is removed (310 bp). Sample genotypes: + indicates the *Tiparp* WT allele; letters indicate the *Tiparp* tm1 corresponding allele (tm1a, tm1b, tm1c, and tm1d).

Mice generated in this study were from ES cell clone G3. Mice harboring the conditional *Tiparp*<sup>fl</sup> allele were generated from the *Tiparp* tm1a allele by excision of the Neo and LacZ genes through crosses with B6(C3)-Tg(Pgk1-FLPo)10Sykr/J mice, leaving the targeted exon flanked by LoxP sites. Mice heterozygous for the tm1c allele were then intercrossed to make homozygous tm1c mice (*Tiparp*<sup>fl/fl</sup>; tm1c allele).

#### Complete and Hepatocyte-Specific Excision of the *Tiparp*<sup>fl/fl</sup> Allele

Using genetraps targeted TIPARP null mice in which a LacZ gene is inserted in front of exon 1 in the *Tiparp* gene (Schmahl et al., 2007), we reported that loss of TIPARP expression increased the sensitivity of mice to dioxin-induced steatohepatitis and lethality (Ahmed et al., 2015). These findings supported the notion that TIPARP protects against dioxin-induced toxicity by negatively regulating AHR action. Because the type of gene knockout targeting strategy can impact the phenotypes observed from targeting the same gene, we created a complete TIPARP knockout by removal of exon 3 of *Tiparp* (*Tiparp*<sup>Ex3-/-</sup>) as described in Materials and Methods section. To generate a complete TIPARP null mouse in which exon 3 is removed (*Tiparp*<sup>Ex3-/-</sup>) we used 2 different strategies. In the first approach, mice heterozygous for the tm1c allele were bred to B6.C-Tg(CMV-cre)1Cgn/J mice to remove the targeted exon (*Tiparp*<sup>Ex3-/-</sup>; tm1d allele). In second approach, mice carrying the tm1a allele were bred to

B6.C-Tg(CMV-cre)1Cgn/J mice to remove the Neo cassette and the targeted exon and leave the lacZ reporter (*Tiparp*<sup>Ex3-/-</sup>; tm1b allele). A map of the *Tiparp* tm1c, tm1d, and tm1b alleles is shown in Figure 1C. The correct genotype was confirmed by PCR analysis of genomic DNA (Figure 1D). *Tiparp*<sup>Ex3-/-</sup> mice represent a distinct TIPARP null strain compared with *Tiparp* targeted knockout using a genetraps approach (Ahmed et al., 2015; Schmahl et al., 2007). To determine whether the loss of TIPARP in hepatocytes is sufficient to increase sensitivity to dioxin-dependent toxicity, we generated mice in which *Tiparp* was deleted in hepatocytes, *Tiparp*<sup>fl/fl</sup>Cre<sup>Alb</sup> (Figure 2A). *Tiparp*<sup>fl/fl</sup>Cre<sup>Alb</sup> mice were created by breeding mice homozygous for the tm1c allele (*Tiparp*<sup>fl/fl</sup>) with B6N.Cg-Tg(Alb-cre)21Mgn/J mice to remove the targeted exon specifically in hepatocytes (Walisser et al., 2005). For the *Tiparp*<sup>fl/fl</sup>Cre<sup>Alb</sup> line, WT mice were referred to as *Tiparp*<sup>fl/fl</sup>, whereas for the *Tiparp*<sup>Ex3-/-</sup> line, WT mice were referred to as *Tiparp*<sup>+/+</sup> for simplicity.

To examine the specificity of excision events in *Tiparp*<sup>fl/fl</sup>Cre<sup>Alb</sup> mice, we analyzed various tissues by determining the relative ratios of *Tiparp* exon 3 compared with intron 1 using qPCR. *Tiparp* exon 3 was efficiently excised in liver tissue and in isolated hepatocytes (Hepa) in the presence of Cre<sup>Alb</sup>, but not in the other tissues examined (Figure 2A). *Tiparp* exon 3 was not detected in liver tissue isolated from *Tiparp*<sup>Ex3-/-</sup> mice (Figure 2B). In the absence of Cre<sup>Alb</sup>, the *Tiparp*<sup>fl/fl</sup> mice showed

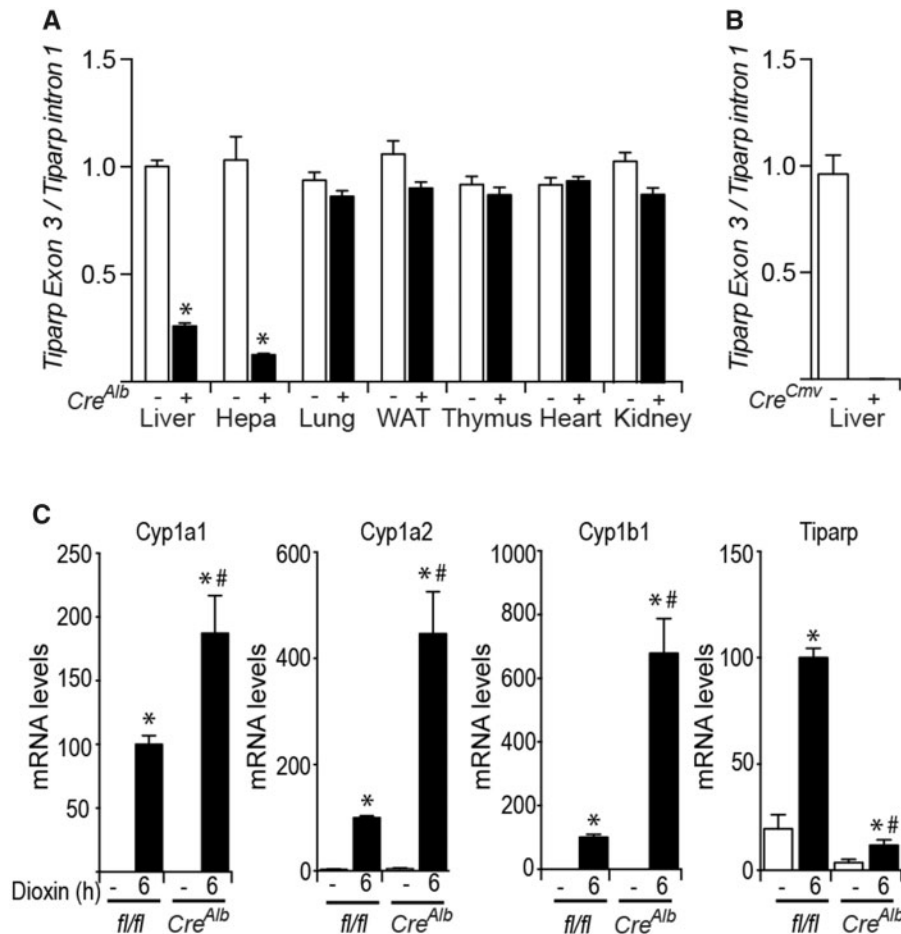


**Figure 2.** Specificity of Cre<sup>Alb</sup>-mediated excision of the *Tiparp*<sup>fl</sup> allele. **A**, Specificity of *Tiparp*<sup>fl</sup> excision by Cre<sup>Alb</sup> was determined by quantitative real-time PCR-based genotyping for excised and unexcised alleles of *Tiparp*<sup>fl</sup> in genomic DNA isolated from various tissues and hepatocytes obtained from *Tiparp*<sup>fl/fl</sup> and *Tiparp*<sup>fl/fl</sup>Cre<sup>Alb</sup> mice. \**p* < .05 compared with tissue matched *Tiparp*<sup>fl/fl</sup> mice. **B**, *Tiparp*<sup>fl</sup> excision by Cre<sup>Cmv</sup> was determined from genomic DNA isolated from livers of *Tiparp*<sup>fl/+</sup> and *Tiparp*<sup>fl/+</sup>Cre<sup>Cmv</sup> mice. Abbreviations: Hep, hepatocytes; WAT, white adipose tissue. **C**, Increased AHR regulated *Cyp1a1*, *Cyp1a2*, *Cyp1b1*, and *Tiparp* mRNA levels in expression in hepatocytes isolated from *Tiparp*<sup>fl/fl</sup> and *Tiparp*<sup>fl/fl</sup>Cre<sup>Alb</sup> mice treated with 10-nM dioxin for 6 h. RNA and qPCR were performed as described in the materials and methods section. \**p* < .05 compared with genotypic match control treated, #*p* < .05 compared with dioxin-treated *Tiparp*<sup>fl/fl</sup> (*n* = 3).

only the *Tiparp*<sup>fl</sup>-unexcised allele in all tissues and isolated hepatocytes examined (Figure 2A).

Cloning and DNA sequencing revealed that the conditional inactivation of the *Tiparp*<sup>fl</sup> allele accomplished by Cre-mediated deletion of exon 3 (169 bp) results in splicing and fusion between exon 2 (961 bp) and exon 4 (161 bp), leading to the insertion of a premature stop codon. This truncated version of TIPARP contains 311 amino acids, of which the last 4 are the result of a frameshift (the full-length protein is 657 a.a.), and it lacks its tryptophan-tryptophan-glutamate (WWE) and catalytic domains (MacPherson et al., 2013). In agreement with a previous study, cloning and transient transfection of the truncated TIPARP protein failed to inhibit AHR-dependent and dioxin-induced CYP1A1 reporter gene activity (Supplementary Figure 1).

Consistent with TIPARP's role as a negative regulator of AHR activity, exposure of hepatocytes from *Tiparp*<sup>fl/fl</sup>Cre<sup>Alb</sup> mice for 6 h to 10 nM dioxin increased mRNA expression levels of the AHR target genes *Cyp1a1*, *Cyp1a2* and *Cyp1b1* compared with similarly treated hepatocytes from *Tiparp*<sup>fl/fl</sup> mice (Figure 2C). *Tiparp* mRNA expression levels were markedly decreased in hepatocytes isolated from *Tiparp*<sup>fl/fl</sup>Cre<sup>Alb</sup> mice compared with *Tiparp*<sup>fl/fl</sup> mice. We next examined the effect of TIPARP loss on AHR target gene expression in liver and lung tissues isolated from

*Tiparp*<sup>Ex3-/-</sup>, *Tiparp*<sup>fl/fl</sup>Cre<sup>Alb</sup>, and WT mice 6 h after treatment with 100 μg/kg dioxin. Higher *Cyp1a1* and *Cyp1b1* mRNA levels were observed in both liver and lung from *Tiparp*<sup>Ex3-/-</sup> mice than in *Tiparp*<sup>Ex3+/+</sup> mice (Figs. 3A and 3B). *Tiparp* mRNA levels were not detected in liver or lung from *Tiparp*<sup>Ex3-/-</sup> mice compared with *Tiparp*<sup>+/+</sup> mice (Figure 3C). Significantly increased dioxin-induced *Cyp1a1* and *Cyp1b1* mRNA levels above those observed in *Tiparp*<sup>fl/fl</sup> mice were only observed in liver and lung from *Tiparp*<sup>fl/fl</sup>Cre<sup>Alb</sup> mice (Figs. 3D and 3E). As expected, TIPARP expression levels were reduced in liver, but not in lung of *Tiparp*<sup>fl/fl</sup>Cre<sup>Alb</sup> compared with *Tiparp*<sup>fl/fl</sup> mice (Figure 3F).

#### ***Tiparp*<sup>Ex3-/-</sup> Mice Exhibit Increased Sensitivity to Dioxin-Induced Toxicity and Lethality**

To determine the sensitivity of *Tiparp*<sup>Ex3-/-</sup> mice to dioxin-induced toxicity, these mice and their respective WT controls were injected with a single dose of 10 or 100 μg/kg dioxin and monitored for up to 30 days, as previously described (Ahmed et al., 2015). All *Tiparp*<sup>Ex3+/+</sup> mice were normal in physical appearance at the end of the 30-day observation period (Figure 4A), while no dioxin-treated *Tiparp*<sup>Ex3-/-</sup> mice (tm1d or tm1b) survived the 30-day experiment (Figure 4A). *Tiparp*<sup>Ex3-/-</sup> mice treated with 100 μg/kg dioxin became weakened and

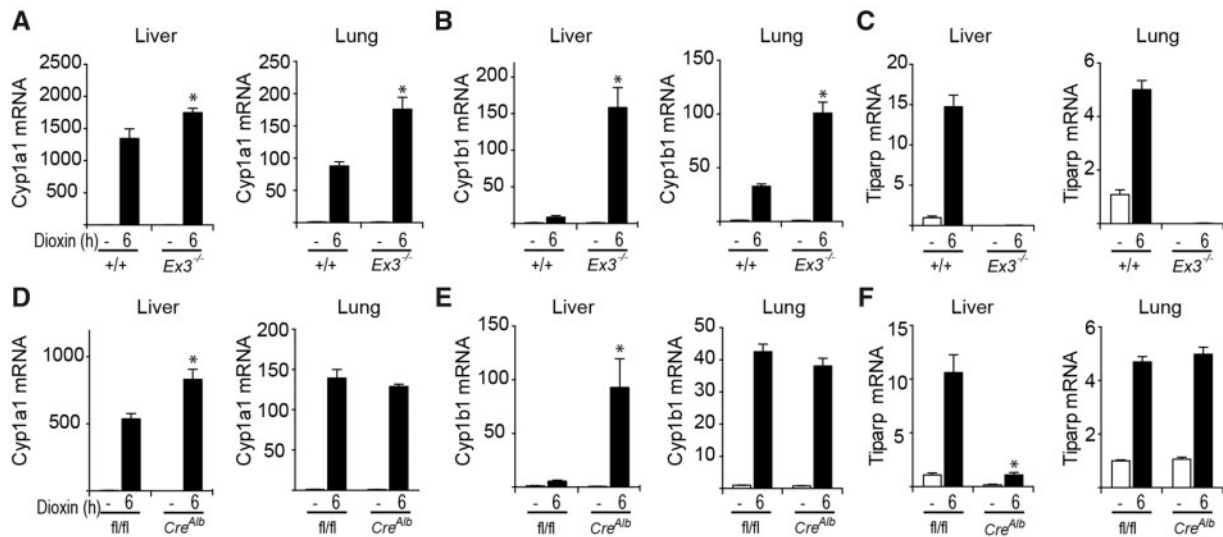


**Figure 3.** AHR regulated transcript levels in liver and lung tissue isolate from control and dioxin-treated *Tiparp*<sup>Ex3<sup>-/-</sup>, *Tiparp*<sup>fl/fl</sup>*Cre*<sup>Alb</sup>, and their respective WT mice. Mice were treated with a single injection of 100  $\mu$ g/kg dioxin in DMSO, or DMSO vehicle alone, and euthanized 6 h later. RNA and qPCR were performed as described in the Materials and Methods section. \**p* < .05 compared with genotype matched control-treated; #*p* < .05 compared with dioxin-treated *Tiparp*<sup>+/+</sup> (A–C) or *Tiparp*<sup>fl/fl</sup> (D–F) (*n* = 4).</sup>

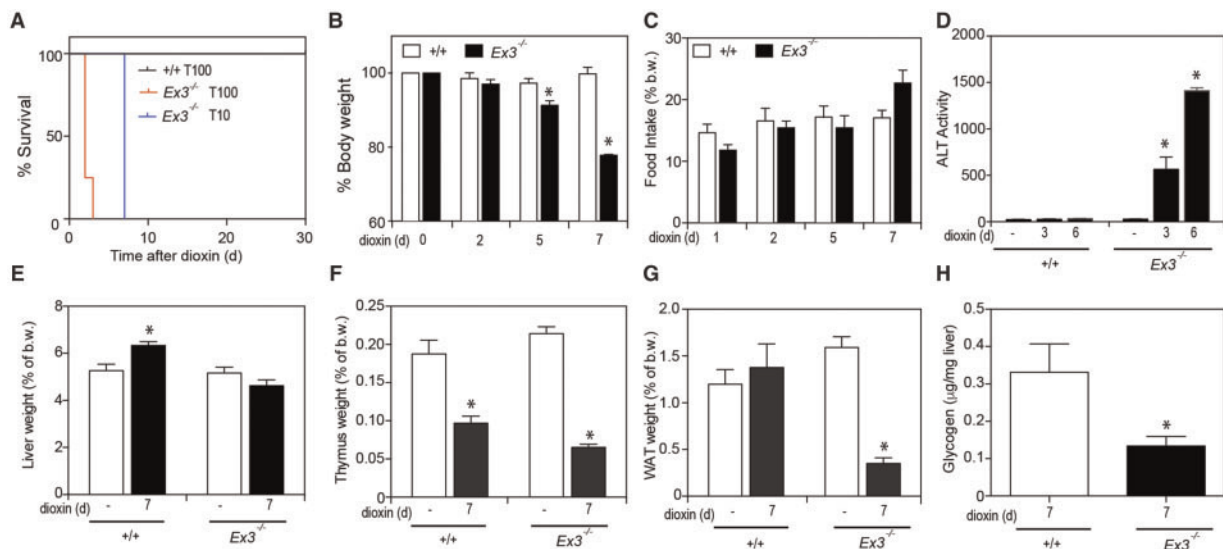


**Figure 4.** Loss of TIPARP increases dioxin-induced hepatotoxicity and lethal wasting syndrome in male mice. A, Kaplan-Meier survival curves for male *Tiparp*<sup>+/+</sup> and *Tiparp*<sup>Ex3<sup>-/-</sup> mice treated with a single 10 or 100  $\mu$ g/kg i.p. injection of dioxin and monitored for 30 days. B, Body weight, (C) food intake, (D) serum ALT activity, (E) liver, (F) thymus, and (G) WAT weight expressed as percentage of total body weight, and (H) hepatic glycogen levels were measured from *Tiparp*<sup>+/+</sup> and *Tiparp*<sup>Ex3<sup>-/-</sup> mice treated with 10  $\mu$ g/kg dioxin. Data shown are the mean  $\pm$  SEM (*n* = 4–5). For (B–G) \**p* < .05, 2-way ANOVA followed by Tukey's post hoc test compared with genotype-matched control treated mice. For (H) \**p* < .05, Student's *t* test.</sup></sup>

moribund and were humanely euthanized between days 2 and 3, while those treated with 10  $\mu$ g/kg dioxin were euthanized at day 7. *Tiparp*<sup>Ex3<sup>-/-</sup> mice treated with 10  $\mu$ g/kg dioxin had lost significant body weight by 5 days after treatment (Figure 4B); however, no decrease in food intake was observed (Figure 4C). No changes in food intake or body weight were seen in dioxin-exposed *Tiparp*<sup>+/+</sup> mice. Serum ALT activity, a marker of hepatotoxicity, was significantly increased in dioxin-treated *Tiparp*<sup>Ex3<sup>-/-</sup> mice, while no increase above controls was observed in *Tiparp*<sup>+/+</sup> mice (Figure 4D). Increased liver weight was observed in dioxin-treated *Tiparp*<sup>+/+</sup> mice but not in *Tiparp*<sup>Ex3<sup>-/-</sup> mice (Figure 4E). Thymic involution, an endpoint associated with dioxin toxicity, responded as expected in both genotypes at day 7 (Figure 4F). A</sup></sup></sup>

significant decrease in epididymal WAT weight was seen in *Tiparp*<sup>Ex3<sup>-/-</sup> mice but not in WT mice (Figure 4G). No differences in BAT weight were observed (data not shown). Hepatic glycogen stores were lower in dioxin-treated *Tiparp*<sup>Ex3<sup>-/-</sup> mice than in WT mice (Figure 4H). These data support the importance of TIPARP in regulating AHR action and show that loss of its expression in mice increases their sensitivity to dioxin toxicity.</sup></sup>

#### Hepatocyte-Specific Loss of TIPARP Results in Increased Sensitivity to Dioxin-Induced Toxicity and Lethality

Because AHR expression in hepatocytes is required for dioxin-induced liver toxicity, we hypothesized that the loss of TIPARP expression in hepatocytes would enhance dioxin-dependent

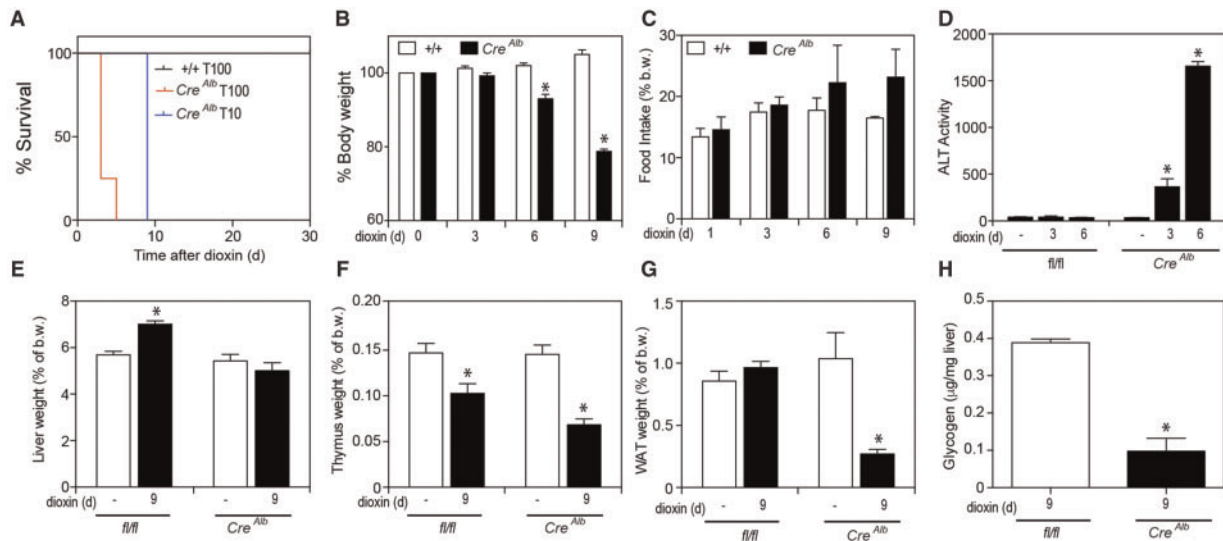


**Figure 5.** Hepatocyte-specific loss of TIPARP increases dioxin-induced hepatotoxicity and lethal wasting syndrome in male mice. **A**, Kaplan-Meier survival curves for male *Tiparp<sup>fl/fl</sup>* and *Tiparp<sup>fl/fl</sup>Cre<sup>Alb</sup>* mice treated with a single 10 or 100  $\mu\text{g}/\text{kg}$  i.p. injection of dioxin and monitored for 30 days. **B**, Body weight, **(C)** food intake, **(D)** serum ALT activity, **(E)** liver, **(F)** thymus, **(G)** WAT weight expressed as percentage of total body weight, and **(H)** hepatic glycogen levels were measured from *Tiparp<sup>fl/fl</sup>* and *Tiparp<sup>fl/fl</sup>Cre<sup>Alb</sup>* mice treated with 10  $\mu\text{g}/\text{kg}$  dioxin. Data shown are the mean  $\pm$  SEM ( $n = 4$ –5). For **(B–G)**  $p < .05$ , 2-way ANOVA followed by Tukey's post hoc test compared with genotype-matched control treated mice. For **(H)**  $*p < .05$ , Student's *t* test.

liver toxicity. To test this hypothesis, we treated *Tiparp<sup>fl/fl</sup>Cre<sup>Alb</sup>* and *Tiparp<sup>fl/fl</sup>* mice with a single i.p. injection of 10 or 100  $\mu\text{g}/\text{kg}$  dioxin and monitored the mice for up to 30 days. As expected, all *Tiparp<sup>fl/fl</sup>* mice were normal in physical appearance at the end of the 30-day observation period (Figure 5A). No dioxin-treated *Tiparp<sup>fl/fl</sup>Cre<sup>Alb</sup>* mice survived the 30-day experiment (Figure 5A). *Tiparp<sup>fl/fl</sup>Cre<sup>Alb</sup>* mice treated with 100  $\mu\text{g}/\text{kg}$  dioxin appeared weakened and moribund and were humanely euthanized between days 3 and 5, while those treated with 10  $\mu\text{g}/\text{kg}$  dioxin were humanely euthanized at day 9. Sensitivity to dioxin-induced lethality was significantly different between *Tiparp<sup>fl/fl</sup>Cre<sup>Alb</sup>* and *Tiparp<sup>Ex3-/-</sup>* mice at both 10 and 100  $\mu\text{g}/\text{kg}$  dioxin, suggesting that cells other than hepatocytes also contribute to dioxin lethality in these models. *Tiparp<sup>fl/fl</sup>Cre<sup>Alb</sup>* mice treated with 10  $\mu\text{g}/\text{kg}$  dioxin had lost significant body weight by 6 days after treatment (Figure 5B), while no decrease in food intake was observed (Figure 5C). No change in food intake or body weight was seen in *Tiparp<sup>fl/fl</sup>* mice. Serum ALT was significantly increased in dioxin-treated *Tiparp<sup>fl/fl</sup>Cre<sup>Alb</sup>* mice at days 3 and 6, but no increase was observed in *Tiparp<sup>fl/fl</sup>* mice (Figure 5D). Increased liver weight was observed in dioxin-treated *Tiparp<sup>fl/fl</sup>* mice but not in *Tiparp<sup>fl/fl</sup>Cre<sup>Alb</sup>* mice (Figure 5E). Decreased thymus weight was seen in both genotypes at day 9 (Figure 5F). Consistent with dioxin-treated *Tiparp<sup>Ex3-/-</sup>* mice, *Tiparp<sup>fl/fl</sup>Cre<sup>Alb</sup>* mice had significantly decreased epididymal WAT levels compared with WT mice (Figure 5G). No difference in BAT weight was observed (data not shown). Hepatic glycogen stores were also decreased in dioxin-treated *Tiparp<sup>fl/fl</sup>Cre<sup>Alb</sup>* mice compared with *Tiparp<sup>fl/fl</sup>* mice (Figure 5H). These findings show that hepatocyte-specific deletion of TIPARP is sufficient to increase dioxin-induced toxicity and lethality.

As an independent measure of liver toxicity, livers were sectioned and stained with hematoxylin and eosin. Vehicle-treated *Tiparp<sup>fl/fl</sup>* and *Tiparp<sup>fl/fl</sup>Cre<sup>Alb</sup>* mice had histologically normal liver architecture (Figure 6A). On day 9, dioxin-treated *Tiparp<sup>fl/fl</sup>* livers exhibited slight hepatocyte cytoplasmic clearing within periportal regions and inflammatory cell infiltration (Figure 6A). In

contrast, day 9 *Tiparp<sup>fl/fl</sup>Cre<sup>Alb</sup>* livers were characterized by inflammatory infiltration and a predominant microvesicular steatosis. Six days after dioxin treatment, livers from *Tiparp<sup>fl/fl</sup>* mice displayed distinct inflammatory cell infiltration and increased clearing of the cytoplasm with the appearance of large vacuoles within hepatocytes. Similar findings were observed in livers isolated from dioxin-treated *Tiparp<sup>+/+</sup>* and *Tiparp<sup>Ex3-/-</sup>* mice (Supplementary Figure 2A).

We next determined the mRNA levels of AHR-regulated cytokines and the macrophage marker F4/80 (Casado et al., 2011; Matsubara et al., 2012). Hepatic interleukin 6 (Il6) levels were unaffected by dioxin treatment in both genotypes (Figure 6B). However, dioxin-treated *Tiparp<sup>fl/fl</sup>Cre<sup>Alb</sup>* mice had increased hepatic expression of *Serpine 1* (also known as plasminogen activator inhibitor-1; PAI-1), chemokine (C-X-C motif) ligand 2 (*Cxcl2*) and F4/80 when compared with *Tiparp<sup>fl/fl</sup>* mice (Figs. 6C–E). Similar findings were also seen in livers isolated from dioxin-treated *Tiparp<sup>+/+</sup>* and *Tiparp<sup>Ex3-/-</sup>* mice (Supplementary Figs. 2B–E). The increased cytokine and F4/80 levels indicated increased hepatic inflammation in dioxin-treated *Tiparp<sup>fl/fl</sup>Cre<sup>Alb</sup>* compared with WT mice.

#### Hepatocyte-Specific Loss of TIPARP Increases Dioxin-Induced Steatohepatitis

Livers from vehicle-treated *Tiparp<sup>fl/fl</sup>* and *Tiparp<sup>fl/fl</sup>Cre<sup>Alb</sup>* mice were macroscopically normal (Figure 7A). Livers from *Tiparp<sup>fl/fl</sup>* mice were enlarged but only slightly pale in color 9 days after dioxin treatment (Figure 7A). Livers from dioxin-treated *Tiparp<sup>fl/fl</sup>Cre<sup>Alb</sup>* mice were markedly pale in color at 9 days, suggesting a high level of lipid accumulation. We tested for the presence of neutral lipids by Oil-Red-O staining (Figure 7B). Livers from vehicle-exposed *Tiparp<sup>fl/fl</sup>* and *Tiparp<sup>fl/fl</sup>Cre<sup>Alb</sup>* mice were negative for Oil-Red-O staining. On day 9 after dioxin treatment, small droplets of lipid were seen in the livers of *Tiparp<sup>fl/fl</sup>* mice, while those from similarly treated *Tiparp<sup>fl/fl</sup>Cre<sup>Alb</sup>* mice had substantial intracytoplasmic lipid accumulation. Comparable findings were observed in livers isolated from dioxin-treated *Tiparp<sup>+/+</sup>* and *Tiparp<sup>Ex3-/-</sup>* mice (Supplementary Figs. 3A and 3B).



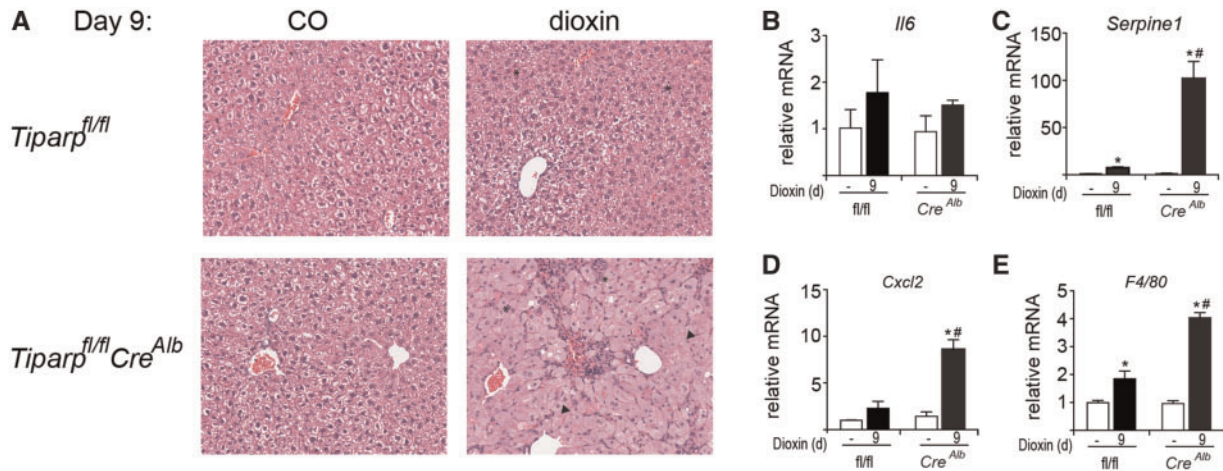


**Figure 6.** Increased liver inflammation and cytokine levels in dioxin-treated *Tiparp<sup>fl/fl</sup>Cre<sup>Alb</sup>* compared with *Tiparp<sup>fl/fl</sup>* mice. **A**, Representative H&E staining of livers from *Tiparp<sup>fl/fl</sup>* and *Tiparp<sup>fl/fl</sup>Cre<sup>Alb</sup>* mice ( $n = 4$ ). Control animals were injected with CO and were euthanized on day 9. The asterisks (\*) indicate focal inflammatory infiltration, and the arrowheads indicate microvesicular steatosis. All images are to the same scale. Hepatic **(B)** *Il6*, **(C)** *Serpine 1*, **(D)** *Cxcl2*, and **(E)** *F4/80* mRNA levels were determined as described in the methods. Data represent the mean  $\pm$  SEM ( $n = 4$ ). \* $p < .05$  2-way ANOVA compared with genotyped-matched control treated mice. # $p < 0.05$  2-way ANOVA compared with dioxin-treated *Tiparp<sup>fl/fl</sup>* mice.

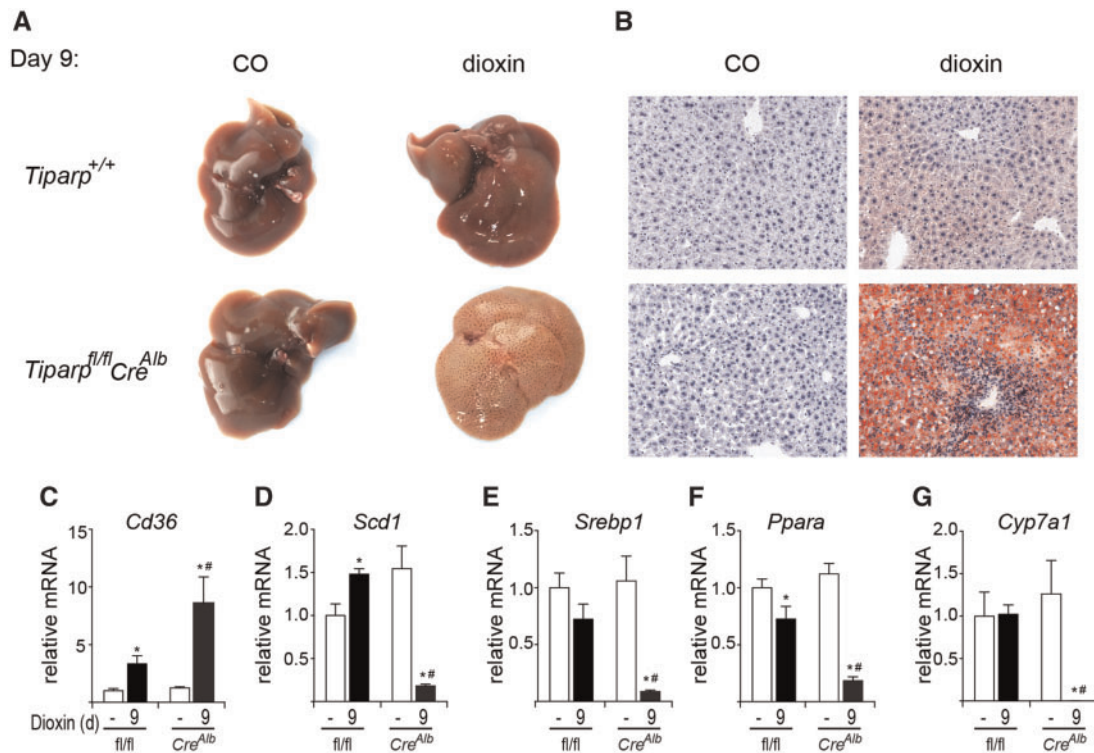


**Figure 7.** Dioxin-induced steatosis is increased in *Tiparp<sup>fl/fl</sup>Cre<sup>Alb</sup>* mice. **(A)** Livers from male *Tiparp<sup>fl/fl</sup>* and *Tiparp<sup>fl/fl</sup>Cre<sup>Alb</sup>* mice given a single i.p. injection of CO or 10  $\mu\text{g}/\text{kg}$  dioxin and euthanized after 9 days ( $n = 5$ ). **B**, Oil-Red-O and hematoxylin stained liver sections from *Tiparp<sup>fl/fl</sup>* and *Tiparp<sup>fl/fl</sup>Cre<sup>Alb</sup>* mice. All images are to the same scale. Hepatic mRNA levels of *Cd36* **(C)**, *Scd1* **(D)**, *Srebp1* **(E)**, *Ppara* **(F)**, and *Cyp7a1* **(G)** were determined as described in the methods. Data represent the mean  $\pm$  SEM ( $n = 4$ ). For all data,  $p < .05$  was determined by 2-way ANOVA followed by Tukey's post hoc test comparison. Significantly different compared with genotype-matched DMSO- or #dioxin-treated *Tiparp<sup>fl/fl</sup>* mice.

We then analyzed the hepatic levels of transcripts encoding genes involved in lipid uptake, lipogenesis and cholesterol/bile acid metabolism. Consistent with previous studies (Lee et al., 2010; Lu et al., 2011), the lipid uptake transporter, scavenger receptor encoded by cluster of differentiation 36 (*Cd36*), was increased 3-fold by dioxin treatment in *Tiparp<sup>fl/fl</sup>* mice and to a

greater extent (8-fold) in similarly treated *Tiparp<sup>fl/fl</sup>Cre<sup>Alb</sup>* mice (Figure 7C). Hepatic expression of lipogenic genes including sterol regulatory element-binding transcription factor 1 (*Srebp1*), and stearoyl-CoA desaturase (*Scd1*) were significantly decreased in dioxin treated *Tiparp<sup>fl/fl</sup>Cre<sup>Alb</sup>* mice compared with *Tiparp<sup>fl/fl</sup>* mice (Figs. 7D and 7E). Peroxisome proliferator activating



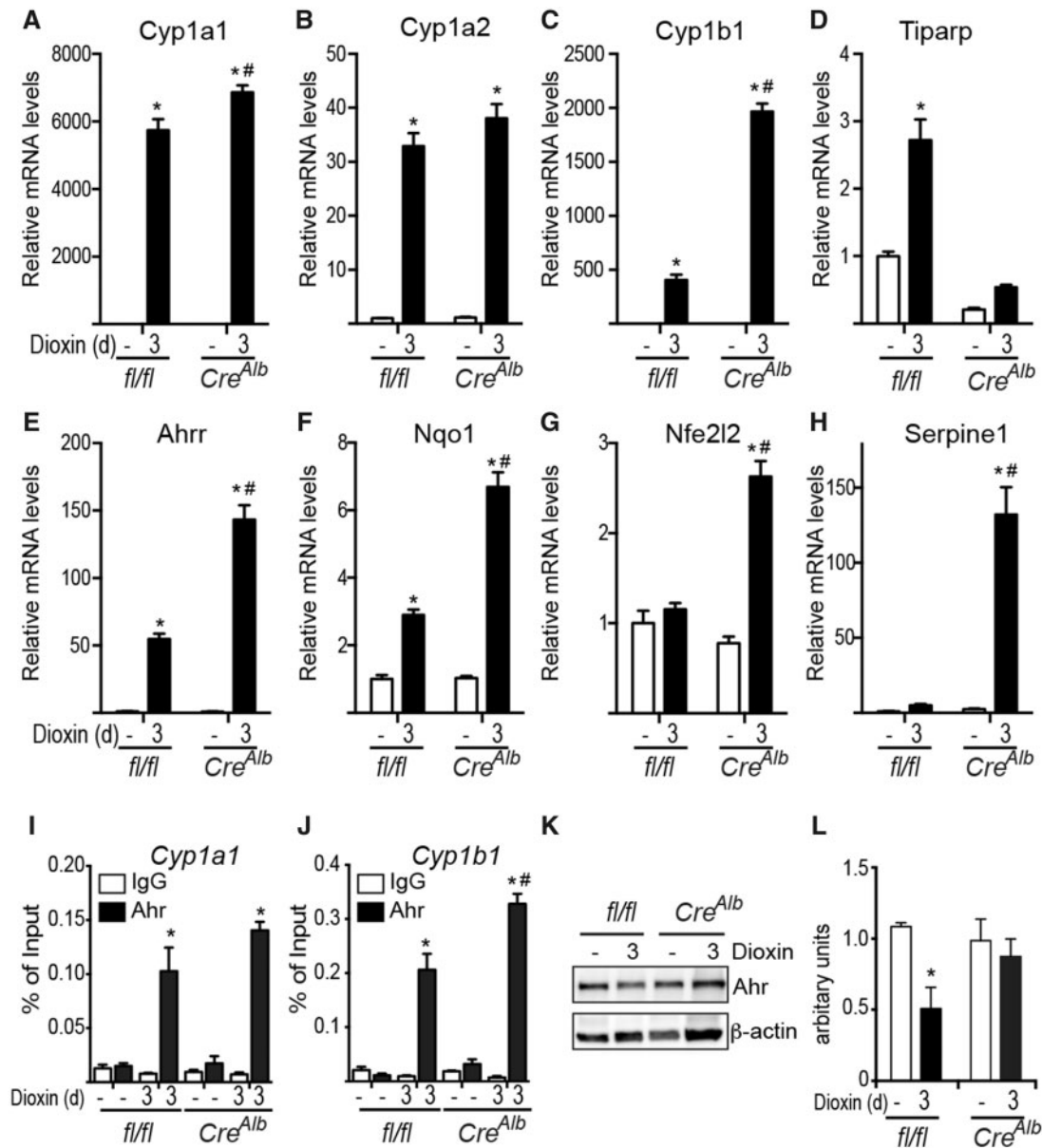


**Figure 8.** Hepatocyte-specific loss of TIPARP increases dioxin-dependent regulation of hepatic AHR target gene expression. Hepatic mRNA levels of *Cyp1a1* (A), *Cyp1a2* (B), *Cyp1b1* (C), *Tiparp* (D), *Ahr* (E), *Nqo1* (F), *Nfe2l2* (G), *Serpine1* (H) were determined after 3 days of exposure to CO or 10  $\mu\text{g}/\text{kg}$  dioxin as described in experimental procedures ( $n = 4$ ). Recruitment of AHR to *Cyp1a1* (I) and *Cyp1b1* (J). Data represent the mean  $\pm$  SEM. Representative AHR (K), and  $\beta$ -actin protein levels were detected by Western blotting after 3 days of treatment. AHR protein levels were normalized to  $\beta$ -actin levels,  $n = 4$  (L). For all data,  $p < .05$  was determined by 2-way ANOVA followed by Tukey's post hoc test comparison. Significantly different compared with genotype-matched \*DMSO- or #dioxin-treated *Tiparp*<sup>fl/fl</sup> mice.

receptor  $\alpha$  (*Ppara*) and *Cyp7a1*, the rate limiting enzyme bile acid synthesis, were also significantly decreased in *Tiparp*<sup>fl/fl</sup>*Cre*<sup>Alb</sup> mice compared with *Tiparp*<sup>fl/fl</sup> mice (Figs. 7F and 7G). Similar findings were seen in livers isolated from dioxin-treated *Tiparp*<sup>+/+</sup> and *Tiparp*<sup>Ex3-/-</sup> mice (Supplementary Figs. 3C–G). These data suggest that the increased sensitivity of *Tiparp*<sup>fl/fl</sup>*Cre*<sup>Alb</sup> and *Tiparp*<sup>Ex3-/-</sup> mice to dioxin-induced steatohepatitis is due to increased lipid uptake rather than increased hepatic lipogenesis.

#### Increased AHR Regulated Gene Expression in *Tiparp*<sup>fl/fl</sup>*Cre*<sup>Alb</sup> Mice After Treatment With 10 $\mu\text{g}/\text{kg}$ Dioxin

To identify AHR genes and/or changes in metabolites that might provide insight into the molecular mechanisms regulating the increased dioxin sensitivity of *Tiparp*<sup>fl/fl</sup>*Cre*<sup>Alb</sup> mice, we analyzed

changes in dioxin-induced hepatic mRNA and metabolite levels 3 days after dioxin treatment. Day 3 was chosen because we observed significant increases in serum ALT activity in *Tiparp*<sup>fl/fl</sup>*Cre*<sup>Alb</sup> mice, and we reasoned that this time point could be used to identify early changes in AHR target gene expression and/or metabolite levels prior to more severe toxicities that ultimately led to death. *Tiparp*<sup>fl/fl</sup>*Cre*<sup>Alb</sup> mice treated with 10  $\mu\text{g}/\text{kg}$  dioxin exhibited increased mRNA expression levels of many AHR target genes including *Cyp1a1*, *Cyp1a2*, *Ahr*, *Nqo1*, *Nfe2l2* and *Serpine1* compared with similarly treated *Tiparp*<sup>fl/fl</sup> mice (Figs. 8A and 8C–H). *Cyp1a2* expression was slightly increased in *Tiparp*<sup>fl/fl</sup>*Cre*<sup>Alb</sup> compared with *Tiparp*<sup>fl/fl</sup> mice, but this difference was not statistically significant (Figure 8B). No significant increase in AHR recruitment to *Cyp1a1* was observed (Figure 8I).

Significantly higher levels of AHR were recruited to Cyp1b1 in liver extracts from *Tiparp<sup>fl/fl</sup>Cre<sup>Alb</sup>* mice compared with *Tiparp<sup>fl/fl</sup>* mice (Figure 8J). Consistent with our previous study, we observed reduced dioxin-induced proteolytic degradation of total AHR protein in liver extracts from *Tiparp<sup>fl/fl</sup>Cre<sup>Alb</sup>* mice compared with *Tiparp<sup>fl/fl</sup>* mice (Figure 8K).

We next did comparative metabolomic analyses on liver extracts from *Tiparp<sup>fl/fl</sup>Cre<sup>Alb</sup>* and *Tiparp<sup>fl/fl</sup>* mice. Principal component analysis (PCA) revealed significant treatment-based separations among the samples, with clear distinctions between the vehicle- and dioxin-treated animals in each genotype. Separations were also apparent between the dioxin-treated *Tiparp<sup>fl/fl</sup>* and *Tiparp<sup>fl/fl</sup>Cre<sup>Alb</sup>* animals (Figure 9A). Of the total of 679 named metabolites examined, 213 were significantly altered ( $P < 0.05$ ) by dioxin treatment of *Tiparp<sup>fl/fl</sup>Cre<sup>Alb</sup>* mice compared with 124 in similarly treated *Tiparp<sup>fl/fl</sup>* mice (Table 1; Supplementary Tables 2 and 3). Of the 124 metabolites, 74 overlapped with those identified in dioxin-treated *Tiparp<sup>fl/fl</sup>Cre<sup>Alb</sup>* mice (Figure 9B). Only 7 metabolites were significantly changed in vehicle-treated *Tiparp<sup>fl/fl</sup>Cre<sup>Alb</sup>* compared with *Tiparp<sup>fl/fl</sup>* mice, showing that the loss of TIPARP had little effect on basal liver metabolism (Supplementary Table 4). Consistent with previous studies, dioxin treatment resulted in significant lipidomic changes, with accumulation of several classes of free fatty acids and metabolites linked to complex lipid homeostasis (Nault et al., 2016b). Increased lipids were observed in both the *Tiparp<sup>fl/fl</sup>* and *Tiparp<sup>fl/fl</sup>Cre<sup>Alb</sup>* animals, with a few classes of lipids that were differentially expressed in the 2 groups (Supplementary Tables 2 and 3). These included certain long-chain acylcarnitines, fatty acid dicarboxylates, and complex lipids such as plasmalogens and sphingolipids. However, 129 metabolites were altered in dioxin-treated *Tiparp<sup>fl/fl</sup>Cre<sup>Alb</sup>* compared with *Tiparp<sup>fl/fl</sup>* mice (Table 1; Supplementary Table 5). Altered metabolite levels in *Tiparp<sup>fl/fl</sup>Cre<sup>Alb</sup>* and *Tiparp<sup>fl/fl</sup>* mice were analyzed for pathway overrepresentation (enrichment) and connectivity within related metabolites (impact) using MetaboAnalyst (Xia and Wishart, 2016) (Figs. 9C and 9D). Only glycerophospholipid metabolism was common among the top 5 or 6 significant pathways (Supplementary Tables 6 and 7). Dioxin-treated *Tiparp<sup>fl/fl</sup>Cre<sup>Alb</sup>* mice also differed with regard to increased  $\gamma$ -glutamyl- $\epsilon$ -lysine levels (12.5-fold; Figure 9E), which may reflect increased transglutaminase activity, and polyamine metabolism (N-acetylputrescine; Figure 9F, and putrescine; Figure 9G). Because dioxin toxicity has been tightly linked with NAD<sup>+</sup> levels, its precursors and metabolites, and because TIPARP activity is dependent on NAD<sup>+</sup>, we examined NAD<sup>+</sup> metabolism (Diani-Moore et al., 2010, 2017; He et al., 2013). Dioxin-dependent increases in nicotinamide ribonucleoside (Figure 9H) and nicotinamide (Figure 9I) were observed in *Tiparp<sup>fl/fl</sup>Cre<sup>Alb</sup>* and *Tiparp<sup>fl/fl</sup>* mice, respectively. Significant decreases in intrahepatic NAD<sup>+</sup> levels were only observed in dioxin-treated *Tiparp<sup>fl/fl</sup>Cre<sup>Alb</sup>* mice (Figure 9J).

## DISCUSSION

We previously reported that TIPARP acts as part of negative feedback loop to regulate AHR activity, and that global loss of TIPARP expression increases sensitivity to dioxin-induced toxicities such as steatohepatitis and wasting syndrome (Ahmed et al., 2015; MacPherson et al., 2013). Since hepatocyte-specific deletion of AHR prevents dioxin-induced hepatotoxicity, we reasoned that hepatocyte-specific deletion of TIPARP would result in increased dioxin-induced hepatotoxicity. We therefore generated a hepatocyte-specific TIPARP deletion (*Tiparp<sup>fl/fl</sup>Cre<sup>Alb</sup>*) mouse strain. We also generated a whole-body knockout

TIPARP (*Tiparp<sup>Ex3-/-</sup>*) strain in which *Tiparp* is deleted by the removal of exon 3, making it distinct from other TIPARP null lines (Ahmed et al., 2015; Kozaki et al., 2017; Schmahl et al., 2007). Here we show that *Tiparp<sup>Ex3-/-</sup>* and *Tiparp<sup>fl/fl</sup>Cre<sup>Alb</sup>* mice are both more sensitive than WT mice to dioxin-induced hepatotoxicity and lethality. These findings provide further support for the importance of TIPARP in AHR signaling and for its role in protecting against dioxin-induced toxicity (Ahmed et al., 2015; Matthews, 2017), as well as demonstrating that the expression of TIPARP in hepatocytes plays a key role in the manifestations of this toxicity.

*Tiparp<sup>fl/fl</sup>Cre<sup>Alb</sup>* mice treated with dioxin lost significant body weight without any reduction in food intake. Hepatic glycogen and epididymal WAT levels were also reduced, pointing to a possible deficiency in the efficiency of intestinal nutrient absorption resulting in altered metabolism. Dioxin-induced hypophagia contributes to body weight and adipose tissue loss in many species, but numerous studies using pair-feeding or total parenteral nutrition have failed to identify a single explanation for the weight loss (Linden et al., 2010; Seefeld et al., 1984). The severe hepatotoxicity and extensive hepatosteatosis in dioxin-treated *Tiparp<sup>fl/fl</sup>Cre<sup>Alb</sup>* and *Tiparp<sup>Ex3-/-</sup>* mice, would cause impaired liver function that could result in reduced intestinal nutrient absorption and impaired liver homeostasis (Kalaitzakis, 2014).

Dioxin-treated *Tiparp<sup>fl/fl</sup>Cre<sup>Alb</sup>* and *Tiparp<sup>Ex3-/-</sup>* mice exhibit many of the alterations in lipid homeostasis, increased hepatic inflammation and other toxic endpoints that have been reported in other studies (Boverhof et al., 2006; Duval et al., 2017). *Tiparp<sup>fl/fl</sup>Cre<sup>Alb</sup>* and *Tiparp<sup>Ex3-/-</sup>* mice exhibited increased hepatosteatosis due to increased expression of genes regulating lipid uptake (Cd36), but decreased expression of those involved in fatty acid  $\beta$ -oxidation and *de novo* lipogenesis (Scd1, Srebp1, Ppara) (Ahmed et al., 2015; Duval et al., 2017; Lee et al., 2010). Scd1 expression was increased in *Tiparp<sup>fl/fl</sup>* mice, but decreased in *Tiparp<sup>fl/fl</sup>Cre<sup>Alb</sup>* mice. One possible explanation is that the increased hepatosteatosis in *Tiparp<sup>fl/fl</sup>Cre<sup>Alb</sup>* mice results in negative regulation of Scd1 by other factors or hormones (Mauvoisin and Mounier, 2011). Srebp1 expression levels were decreased in *Tiparp<sup>fl/fl</sup>Cre<sup>Alb</sup>* and *Tiparp<sup>Ex3-/-</sup>* mice, supporting findings from a recent high-dose dioxin exposure study (Duval et al., 2017). Srebp1 expression is positively regulated by the liver X receptor (LXR) and PPAR $\alpha$ . TIPARP is an LXR coactivator, so the loss of *Tiparp* expression combined with the reduced PPAR $\alpha$  expression levels could also contribute to reduced SREBP1 levels (Bindesboll et al., 2016).

CYP7A1 plays a critical role in the control of bile acid and cholesterol homeostasis as the rate-limiting enzyme in the classic bile acid synthesis pathway (Gupta et al., 2001). Overexpression of mouse CYP7A1 protects against high-fat diet induced obesity, fatty liver and insulin resistance (Li et al., 2010), whereas in humans, genetic deficiency of CYP7A1 leads to hyperlipidemia (Pullinger et al., 2002). The decrease in CYP7A1 expression levels in treated *Tiparp<sup>fl/fl</sup>Cre<sup>Alb</sup>* and *Tiparp<sup>Ex3-/-</sup>* mice is in agreement with studies of male C57BL/6 mice treated with 0.01 to 30  $\mu$ g/kg dioxin every 4 for 28 days (Fader et al., 2017), and could be a contributing factor to the increased hepatosteatosis and reduced WAT levels observed, through reduced lipid absorption resulting from altered bile acid homeostasis (Fader et al., 2017). In support of this, we observed increased hepatic levels of taurochenodeoxycholic acid and taurocholic acid in dioxin-treated *Tiparp<sup>fl/fl</sup>Cre<sup>Alb</sup>* mice but not in *Tiparp<sup>fl/fl</sup>* mice.

Metabolomic profiling studies identified significant changes in metabolite levels in dioxin-treated *Tiparp<sup>fl/fl</sup>Cre<sup>Alb</sup>* mice compared with *Tiparp<sup>fl/fl</sup>* mice. Many of the major treatment-based

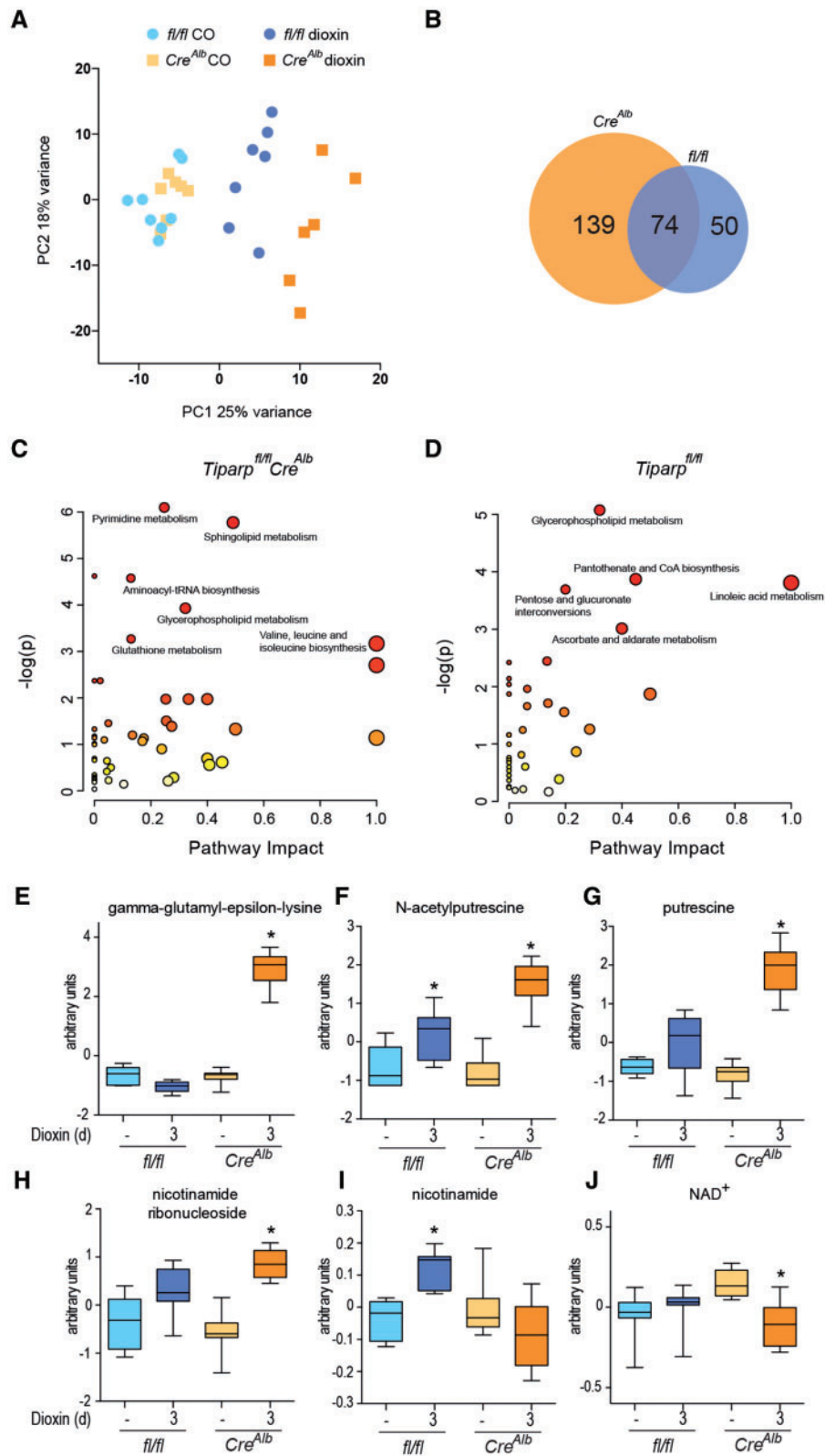


**Figure 9.** Dioxin-induced hepatic metabolomic disruption. A, PCA of hepatic metabolomics after 3-day treatment of  $Tiparp^{fl/fl}$  ( $fl/fl$ ) and  $Tiparp^{fl/fl} Cre^{Alb}$  with CO or 10  $\mu\text{g}/\text{kg}$  dioxin. B, Venn diagram of the overlapping metabolites that were significantly altered between dioxin treated  $Tiparp^{fl/fl}$  and  $Tiparp^{fl/fl} Cre^{Alb}$ . Metabolic pathway enrichment analysis of altered hepatic metabolites ( $p < .05$ ) in dioxin-treated  $Tiparp^{fl/fl} Cre^{Alb}$  (C) and  $Tiparp^{fl/fl}$  mice (D). Hepatic levels of gamma-glutamyl-epsilon lysine (E), N-acetylputrescine (F), putrescine (G), nicotinamide ribonucleoside (H), nicotinamide (I), and  $NAD^+$  (J). Data represent the mean  $\pm$  SEM ( $n = 6-8$ ).



**Table 1.** A Summary of the Numbers of Biochemicals That Achieved Statistical Significance ( $p \leq .05$ ) Among the Different Comparisons

ANOVA contrasts	Statistical Comparisons			
	Tiparp <sup>fl/fl</sup> TCDD Tiparp <sup>fl/fl</sup> CO	Tiparp <sup>fl/fl</sup> Cre <sup>Alb</sup> TCDD Tiparp <sup>fl/fl</sup> Cre <sup>Alb</sup> CO	Tiparp <sup>fl/fl</sup> Cre <sup>Alb</sup> CO Tiparp <sup>fl/fl</sup> CO	Tiparp <sup>fl/fl</sup> Cre <sup>Alb</sup> TCDD Tiparp <sup>fl/fl</sup> TCDD
Total biochemicals ( $p < .05$ )	124	213	7	129
Biochemicals (up   down)	75   49	163   50	4   3	111   18

changes were conserved in the 2 cohorts (ie, accumulated fatty acids, changes related to nucleotides and polyamines). However, the extent of change of the affected metabolites differed between the Tiparp<sup>fl/fl</sup> and Tiparp<sup>fl/fl</sup>Cre<sup>Alb</sup> groups. Dioxin-treated Tiparp<sup>fl/fl</sup>Cre<sup>Alb</sup> mice, however, exhibited significant increases in gamma-glutamyl-epsilon lysine levels compared with their untreated counterparts or dioxin-treated Tiparp<sup>fl/fl</sup> mice. This metabolite is formed by tissue transglutaminase (TG2), which catalyzes cross-links between glutamine and lysine residues of proteins (Iismaa et al., 2009). TG2 activity increases following acute and chronic liver injury, and aberrant TG2 activation has been implicated in the development of fibrosis and cancer (Iismaa et al., 2009). In contrast, retinoid-induced TG2 mRNA up-regulation is reduced by dioxin treatment in a human squamous cell carcinoma cell line (Krig and Rice, 2000). The increased  $\gamma$ -glutamyl- $\epsilon$ -lysine observed in Tiparp<sup>fl/fl</sup>Cre<sup>Alb</sup> mice suggests that TIPARP might influence TG2 activity following dioxin-induced liver damage.

We observed that the expression of most of the AHR target genes examined was increased in response to dioxin in Tiparp<sup>fl/fl</sup>Cre<sup>Alb</sup> and Tiparp<sup>fl/fl</sup> compared with WT mice, including Cxcl2 (macrophage inflammation protein-2) and Serpine1 genes (Son and Rozman, 2002). CXCL2 is a member of the CXC subfamily of chemokines that are crucial for neutrophil recruitment to sites of inflammation following hepatic injury (Marra and Tacke, 2014). Levels of PAI-1, the product of Serpine1 gene, were higher in Tiparp<sup>fl/fl</sup>Cre<sup>Alb</sup> mice than in Tiparp<sup>fl/fl</sup> mice. PAI-1 is a physiologic inhibitor of plasminogen activators that regulate fibrosis via regulation of the extracellular matrix. PAI-1 expression is increased in dioxin-induced fibrosis (Nault et al., 2016a).

The mRNA levels of AHR repressor (AHRR), a negative regulator of AHR (Mimura et al., 1999), were increased in Tiparp<sup>fl/fl</sup>Cre<sup>Alb</sup> compared with Tiparp<sup>fl/fl</sup> mice. AHRR is a potent inhibitor of AHR activity *in vitro* (Karchner et al., 2009) that exhibits gene- and tissue-specific inhibition of AHR signaling in mice (Hosoya et al., 2008). Although the effect of Ahrr loss on dioxin-induced wasting syndrome has not been reported, AHRR transgenic mice are protected from dioxin-induced lethality and hepatotoxicity (Vogel et al., 2016).

Increased TIPARP and PARP1 activity have been proposed to be important in augmenting dioxin toxicity through the depletion of NAD<sup>+</sup>. Indeed, NAD<sup>+</sup> depletion or treatment with the pan-PARP inhibitor PJ34 can prevent dioxin-induced thymic atrophy and hepatosteatosis in a chicken embryo model (Diani-Moore et al., 2017). However, we observed decreased hepatic NAD<sup>+</sup> levels in dioxin-treated Tiparp<sup>fl/fl</sup>Cre<sup>Alb</sup> mice, suggesting that PARP1 or an NAD<sup>+</sup>-consuming enzyme other than TIPARP is responsible for the reduced NAD<sup>+</sup> levels after dioxin treatment in mice. Another possible explanation is that there are species differences in the AHR-TIPARP signaling axis, such that TIPARP protects against dioxin toxicity in mice but enhances it in avian species. Further studies using gene targeting methods to delete TIPARP in nonmurine models are needed to explain these discrepancies.

AHR is also a key regulator of gut homeostasis, inflammation, immunity and T-cell differentiation (Stockinger et al., 2014). AHR is required for the maintenance of intraepithelial lymphocytes,

which are the first line of immune defense in the intestine. Loss of AHR or reduced exposure to dietary AHR ligands compromises these cells, leading to increased microbial load, immune activation and epithelial damage (Li et al., 2011). Moreover, AHR activation by dietary indoles (indole-3-carbinol) improves colitis and protects against experimental autoimmune encephalomyelitis, a murine model of multiple sclerosis (Lamas et al., 2016; Li et al., 2011; Monteleone et al., 2011; Rouse et al., 2013). An unanswered question is whether TIPARP also regulates endogenous AHR signaling and if so, how would its loss affect the protective role of the AHR signaling pathway in models of inflammatory disease? Kynurenine, an endogenous AHR ligand, was reported to repress type-I interferon responses during viral infection in an AHR- and TIPARP-dependent manner, supporting the notion that TIPARP has a broad role in AHR biology and regulates endogenous ligand-induced AHR activation (Yamada et al., 2016).

In summary, we provide evidence from 2 additional mouse models that the loss of TIPARP expression increases sensitivity to dioxin toxicity and lethality. Hepatocyte-specific loss of TIPARP is sufficient to increase sensitivity to dioxin hepatotoxicity, steatosis and lethality, highlighting the importance of liver damage in the dioxin-induced wasting syndrome. Our results provide further support for the importance of the AHR-TIPARP axis in regulating dioxin toxicity, and potentially in regulating the biological actions of AHR following its activation by endogenous or dietary ligands.

## SUPPLEMENTARY DATA

Supplementary data are available at *Toxicological Sciences* online.

## FUNDING

This work was supported by Canadian Institutes of Health Research (CIHR) operating grants (MOP-494265 and MOP-125919), CIHR New Investigator Award, an Early Researcher Award from the Ontario Ministry of Innovation (ER10-07-028), an unrestricted research grant from the DOW Chemical Company, the Johan Throne Holst Foundation, Novo Nordic Foundation and the Norwegian Cancer Society to J.M.

## ACKNOWLEDGMENTS

The authors thank all members of the Matthews and Grant laboratories for their help with the preparation of the article.

## REFERENCES

- Ahmed, S., Bott, D., Gomez, A., Tamblyn, L., Rasheed, A., MacPherson, L., Sugamori, K. S., Cho, T., Yang, Y., Grant, D. M., et al. (2015). Loss of the Mono-ADP-Ribosyltransferase, TIPARP, Increases Sensitivity to Dioxin-Induced Steatohepatitis and Lethality. *J. Biol. Chem.* **290**, 16824–16840.

- Bindesboll, C., Tan, S., Bott, D., Cho, T., Tamblyn, L., MacPherson, L., Gronning-Wang, L. M., Nebb, H. I., and Matthews, J. (2016). TCDD-inducible poly-ADP-ribose polymerase (TiPARP/PARP7) mono-ADP-ribosylates and coactivates liver X receptors. *Biochem. J.* **473**, 899–910.
- Birnbaum, L. S. (1994). Endocrine effects of prenatal exposure to PCBs, dioxins, and other xenobiotics: Implications for policy and future research. *Environ. Health Perspect.* **102**, 676–679.
- Birnbaum, L. S. (1995). Developmental effects of dioxins and related endocrine disrupting chemicals. *Toxicol. Lett.* **82–83**, 743–750.
- Boverhof, D. R., Burgoon, L. D., Tashiro, C., Sharratt, B., Chittim, B., Harkema, J. R., Mendrick, D. L., and Zacharewski, T. R. (2006). Comparative toxicogenomic analysis of the hepatotoxic effects of TCDD in Sprague Dawley rats and C57BL/6 mice. *Toxicol. Sci.* **94**, 398–416.
- Casado, F. L., Singh, K. P., and Gasiewicz, T. A. (2011). Aryl hydrocarbon receptor activation in hematopoietic stem/progenitor cells alters cell function and pathway-specific gene modulation reflecting changes in cellular trafficking and migration. *Mol. Pharmacol.* **80**, 673–682.
- Denison, M. S., and Nagy, S. R. (2003). Activation of the aryl hydrocarbon receptor by structurally diverse exogenous and endogenous chemicals. *Annu. Rev. Pharmacol. Toxicol.* **43**, 309–334.
- Diani-Moore, S., Ram, P., Li, X., Mondal, P., Youn, D. Y., Sauve, A. A., and Rifkind, A. B. (2010). Identification of the aryl hydrocarbon receptor target gene TiPARP as a mediator of suppression of hepatic gluconeogenesis by 2, 3, 7, 8-tetrachlorodibenzo-p-dioxin and of nicotinamide as a corrective agent for this effect. *J. Biol. Chem.* **285**, 38801–38810.
- Diani-Moore, S., Shoots, J., Singh, R., Zuk, J. B., and Rifkind, A. B. (2017). NAD(+) loss, a new player in AhR biology: Prevention of thymus atrophy and hepatosteatosis by NAD(+) repletion. *Sci. Rep.* **7**, 2268.
- Duval, C., Teixeira-Clerc, F., Leblanc, A. F., Touch, S., Emond, C., Guerre-Millo, M., Lotersztajn, S., Barouki, R., Aggerbeck, M., and Coumoul, X. (2017). Chronic exposure to low doses of dioxin promotes liver fibrosis development in the C57BL/6J diet-induced obesity mouse model. *Environ. Health Perspect.* **125**, 428–436.
- Fader, K. A., Nault, R., Zhang, C., Kumagai, K., Harkema, J. R., and Zacharewski, T. R. (2017). 2, 3, 7, 8-Tetrachlorodibenzo-p-dioxin (TCDD)-elicited effects on bile acid homeostasis: Alterations in biosynthesis, enterohepatic circulation, and microbial metabolism. *Sci. Rep.* **7**, 5921.
- Fernandez-Salguero, P. M., Hilbert, D. M., Rudikoff, S., Ward, J. M., and Gonzalez, F. J. (1996). Aryl-hydrocarbon receptor-deficient mice are resistant to 2, 3, 7, 8-tetrachlorodibenzo-p-dioxin-induced toxicity. *Toxicol. Appl. Pharmacol.* **140**, 173–179.
- Gupta, S., Stravitz, R. T., Dent, P., and Hylemon, P. B. (2001). Down-regulation of cholesterol 7 $\alpha$ -hydroxylase (CYP7A1) gene expression by bile acids in primary rat hepatocytes is mediated by the c-Jun N-terminal kinase pathway. *J. Biol. Chem.* **276**, 15816–15822.
- He, J., Hu, B., Shi, X., Weidert, E. R., Lu, P., Xu, M., Huang, M., Kelley, E. E., and Xie, W. (2013). Activation of the aryl hydrocarbon receptor sensitizes mice to nonalcoholic steatohepatitis by deactivating mitochondrial sirtuin deacetylase Sirt3. *Mol. Cell Biol.* **33**, 2047–2055.
- Hosoya, T., Harada, N., Mimura, J., Motohashi, H., Takahashi, S., Nakajima, O., Morita, M., Kawachi, S., Yamamoto, M., and Fujii-Kuriyama, Y. (2008). Inducibility of cytochrome P450 1A1 and chemical carcinogenesis by benzo[a]pyrene in AhR repressor-deficient mice. *Biochem. Biophys. Res. Commun.* **365**, 562–567.
- Hottiger, M. O., Hassa, P. O., Luscher, B., Schuler, H., and Koch-Nolte, F. (2010). Toward a unified nomenclature for mammalian ADP-ribosyltransferases. *Trends Biochem. Sci.* **35**, 208–219.
- Iismaa, S. E., Mearns, B. M., Lorand, L., and Graham, R. M. (2009). Transglutaminases and disease: Lessons from genetically engineered mouse models and inherited disorders. *Physiol. Rev.* **89**, 991–1023.
- Kalaitzakis, E. (2014). Gastrointestinal dysfunction in liver cirrhosis. *World J. Gastroenterol.* **20**, 14686–14695.
- Karchner, S. I., Jenny, M. J., Tarrant, A. M., Evans, B. R., Kang, H. J., Bae, I., Sherr, D. H., and Hahn, M. E. (2009). The active form of human aryl hydrocarbon receptor (AHR) repressor lacks exon 8, and its Pro 185 and Ala 185 variants repress both AHR and hypoxia-inducible factor. *Mol. Cell Biol.* **29**, 3465–3467.
- Kozaki, T., Komano, J., Kanbayashi, D., Takahama, M., Misawa, T., Satoh, T., Takeuchi, O., Kawai, T., Shimizu, S., Matsuura, Y., et al. (2017). Mitochondrial damage elicits a TCDD-inducible poly(ADP-ribose) polymerase-mediated antiviral response. *Proc. Natl. Acad. Sci. U.S.A.* **114**, 2681–2686.
- Kraus, W. L., and Hottiger, M. O. (2013). PARP-1 and gene regulation: Progress and puzzles. *Mol. Aspects Med.* **34**, 1109–1123.
- Krig, S. R., and Rice, R. H. (2000). TCDD suppression of tissue transglutaminase stimulation by retinoids in malignant human keratinocytes. *Toxicol. Sci.* **56**, 357–364.
- Lamas, B., Richard, M. L., Leducq, V., Pham, H. P., Michel, M. L., Da Costa, G., Bridonneau, C., Jegou, S., Hoffmann, T. W., Natividad, J. M., et al. (2016). CARD9 impacts colitis by altering gut microbiota metabolism of tryptophan into aryl hydrocarbon receptor ligands. *Nat. Med.* **22**, 598–605.
- Lee, J. H., Wada, T., Febbraio, M., He, J., Matsubara, T., Lee, M. J., Gonzalez, F. J., and Xie, W. (2010). A novel role for the dioxin receptor in fatty acid metabolism and hepatic steatosis. *Gastroenterology* **139**, 653–663.
- Li, T., Owsley, E., Matozel, M., Hsu, P., Novak, C. M., and Chiang, J. Y. (2010). Transgenic expression of cholesterol 7 $\alpha$ -hydroxylase in the liver prevents high-fat diet-induced obesity and insulin resistance in mice. *Hepatology* **52**, 678–690.
- Li, Y., Innocentin, S., Withers, D. R., Roberts, N. A., Gallagher, A. R., Grigorieva, E. F., Wilhelm, C., and Veldhoen, M. (2011). Exogenous stimuli maintain intraepithelial lymphocytes via aryl hydrocarbon receptor activation. *Cell* **147**, 629–640.
- Linden, J., Lensu, S., Tuomisto, J., and Pohjanvirta, R. (2010). Dioxins, the aryl hydrocarbon receptor and the central regulation of energy balance. *Front. Neuroendocrinol.* **31**, 452–478.
- Lo, R., Celius, T., Forgacs, A., Dere, E., MacPherson, L., Zacharewski, T., and Matthews, J. (2011). Identification of aryl hydrocarbon receptor binding targets in mouse hepatic tissue treated with 2, 3, 7, 8-tetrachlorodibenzo-p-dioxin. *Toxicol. Appl. Pharmacol.* doi: 10.1016/j.taap.2011.08.016.
- Lu, H., Cui, W., and Klaassen, C. D. (2011). Nrf2 protects against 2, 3, 7, 8-tetrachlorodibenzo-p-dioxin (TCDD)-induced oxidative injury and steatohepatitis. *Toxicol. Appl. Pharmacol.* **256**, 122–135.
- Ma, Q., Baldwin, K. T., Renzelli, A. J., McDaniel, A., and Dong, L. (2001). TCDD-inducible poly(ADP-ribose) polymerase: A novel response to 2, 3, 7, 8-tetrachlorodibenzo-p-dioxin. *Biochem. Biophys. Res. Commun.* **289**, 499–506.
- MacPherson, L., Tamblyn, L., Rajendra, S., Bralha, F., McPherson, J. P., and Matthews, J. (2013). 2, 3, 7, 8-tetrachlorodibenzo-p-dioxin poly(ADP-ribose) polymerase (TiPARP, ARTD14) is a mono-ADP-ribosyltransferase and repressor of aryl

- hydrocarbon receptor transactivation. *Nucleic Acids Res.* **41**, 1604–1621.
- Marra, F., and Tacke, F. (2014). Roles for chemokines in liver disease. *Gastroenterology* **147**, 577–594 e1.
- Matsubara, T., Tanaka, N., Krausz, K. W., Manna, S. K., Kang, D. W., Anderson, E. R., Luecke, H., Patterson, A. D., Shah, Y. M., and Gonzalez, F. J. (2012). Metabolomics identifies an inflammatory cascade involved in dioxin- and diet-induced steatohepatitis. *Cell Metab.* **16**, 634–644.
- Matthews, J. (2017). AHR Toxicity and Signalling: Role of TIPARP and ADP-ribosylation. *Curr. Opin. Toxicol.* **2**, 50–57.
- Mauvoisin, D., and Mounier, C. (2011). Hormonal and nutritional regulation of SCD1 gene expression. *Biochimie* **93**, 78–86.
- Mimura, J., Ema, M., Sogawa, K., and Fujii-Kuriyama, Y. (1999). Identification of a novel mechanism of regulation of Ah (dioxin) receptor function. *Genes Dev.* **13**, 20–25.
- Monteleone, I., Rizzo, A., Sarra, M., Sica, G., Sileri, P., Biancone, L., MacDonald, T. T., Pallone, F., and Monteleone, G. (2011). Aryl hydrocarbon receptor-induced signals up-regulate IL-22 production and inhibit inflammation in the gastrointestinal tract. *Gastroenterology* **141**, 237–248, 248 e1.
- Moura-Alves, P., Fae, K., Houthuys, E., Dorhoi, A., Kreuchwig, A., Furkert, J., Barison, N., Diehl, A., Munder, A., Constant, P., et al. (2014). AhR sensing of bacterial pigments regulates anti-bacterial defence. *Nature* **512**, 387–392.
- Nault, R., Fader, K. A., Ammendolia, D. A., Dornbos, P., Potter, D., Sharratt, B., Kumagai, K., Harkema, J. R., Lunt, S. Y., Matthews, J., et al. (2016a). Dose-dependent metabolic reprogramming and differential gene expression in TCDD-elicited hepatic fibrosis. *Toxicol. Sci.* **154**, 253–266.
- Nault, R., Fader, K. A., Kirby, M. P., Ahmed, S., Matthews, J., Jones, A. D., Lunt, S. Y., and Zacharewski, T. R. (2016b). Pyruvate Kinase Isoform Switching and Hepatic Metabolic Reprogramming by the Environmental Contaminant 2, 3, 7, 8-Tetrachlorodibenzo-p-Dioxin. *Toxicol. Sci.* **149**, 358–371.
- Pohjanvirta, R., and Tuomisto, J. (1994). Short-term toxicity of 2, 3, 7, 8-tetrachlorodibenzo-p-dioxin in laboratory animals: Effects, mechanisms, and animal models. *Pharmacol. Rev.* **46**, 483–549.
- Poland, A., and Knutson, J. C. (1982). 2, 3, 7, 8-tetrachlorodibenzo-p-dioxin and related halogenated aromatic hydrocarbons: Examination of the mechanism of toxicity. *Annu. Rev. Pharmacol. Toxicol.* **22**, 517–554.
- Poland, A., Palen, D., and Glover, E. (1994). Analysis of the four alleles of the murine aryl hydrocarbon receptor. *Mol. Pharmacol.* **46**, 915–921.
- Pullinger, C. R., Eng, C., Salen, G., Shefer, S., Batta, A. K., Erickson, S. K., Verhagen, A., Rivera, C. R., Mulvihill, S. J., Malloy, M. J., et al. (2002). Human cholesterol 7 $\alpha$ -hydroxylase (CYP7A1) deficiency has a hypercholesterolemic phenotype. *J. Clin. Invest.* **110**, 109–117.
- Quintana, F. J., Basso, A. S., Iglesias, A. H., Korn, T., Farez, M. F., Bettelli, E., Caccamo, M., Oukka, M., and Weiner, H. L. (2008). Control of T(reg) and T(H)17 cell differentiation by the aryl hydrocarbon receptor. *Nature* **453**, 65–71.
- Rouse, M., Singh, N. P., Nagarkatti, P. S., and Nagarkatti, M. (2013). Indoles mitigate the development of experimental autoimmune encephalomyelitis by induction of reciprocal differentiation of regulatory T cells and Th17 cells. *Br. J. Pharmacol.* **169**, 1305–1321.
- Schmahl, J., Raymond, C. S., and Soriano, P. (2007). PDGF signaling specificity is mediated through multiple immediate early genes. *Nat. Genet.* **39**, 52–60.
- Seefeld, M. D., Corbett, S. W., Keeseey, R. E., and Peterson, R. E. (1984). Characterization of the wasting syndrome in rats treated with 2, 3, 7, 8-tetrachlorodibenzo-p-dioxin. *Toxicol. Appl. Pharmacol.* **73**, 311–322.
- Son, D. S., and Rozman, K. K. (2002). 2, 3, 7, 8-Tetrachlorodibenzo-p-dioxin (TCDD) induces plasminogen activator inhibitor-1 through an aryl hydrocarbon receptor-mediated pathway in mouse hepatoma cell lines. *Arch. Toxicol.* **76**, 404–413.
- Stevens, E. A., Mezrich, J. D., and Bradfield, C. A. (2009). The aryl hydrocarbon receptor: A perspective on potential roles in the immune system. *Immunology* **127**, 299–311.
- Stockinger, B., Di Meglio, P., Gialitakis, M., and Duarte, J. H. (2014). The aryl hydrocarbon receptor: Multitasking in the immune system. *Annu. Rev. Immunol.* **32**, 403.
- Vogel, C. F., Chang, W. L., Kado, S., McCulloh, K., Vogel, H., Wu, D., Haarmann-Stemann, T., Yang, G., Leung, P. S., Matsumura, F., et al. (2016). Transgenic overexpression of aryl hydrocarbon receptor repressor (AhRR) and AhR-mediated induction of CYP1A1, cytokines, and acute toxicity. *Environ. Health Perspect.* **124**, 1071–1083.
- Walisser, J. A., Glover, E., Pande, K., Liss, A. L., and Bradfield, C. A. (2005). Aryl hydrocarbon receptor-dependent liver development and hepatotoxicity are mediated by different cell types. *Proc. Natl. Acad. Sci. U.S.A.* **101**, 16677–16682.
- Whitlock, J. P., Jr. (1999). Induction of cytochrome P4501A1. *Annu. Rev. Pharmacol. Toxicol.* **39**, 103–125.
- Xia, J., and Wishart, D. S. (2016). Using metaboanalyst 3.0 for comprehensive metabolomics data analysis. *Curr. Protoc. Bioinformatics* **55**, 14.10.1.
- Yamada, T., Horimoto, H., Kameyama, T., Hayakawa, S., Yamato, H., Dazai, M., Takada, A., Kida, H., Bott, D., Zhou, A. C., et al. (2016). Constitutive aryl hydrocarbon receptor signaling constrains type I interferon-mediated antiviral innate defense. *Nat. Immunol.* **17**, 687–694.
- Zhang, L., Savas, U., Alexander, D. L., and Jefcoate, C. R. (1998). Characterization of the mouse Cyp1B1 gene. Identification of an enhancer region that directs aryl hydrocarbon receptor-mediated constitutive and induced expression. *J. Biol. Chem.* **273**, 5174–5183.